ORIGINAL ARTICLE

Experimental and predictive study by multi-output fuzzy model of electrical discharge machining performances

Abderrahim Belloufi [1] · Mourad Mezoudj [1] · Mourad Abdelkrim [1] · Imane Rezgui [1] · Elhocine Chiba [1]

Abstract

The nature of electrical discharge machining makes it difficult to predict or even measure machining performance, which is why great attention has been paid to methodologies for measuring these performances. In this work, an experimental approach for measuring machining electrical discharge performance and geometric errors was presented. This can improve the authenticity of the parameters measured. A technique for identifying machining parameters using a multi-output system based on fuzzy logic has been proposed. The objective was to determine the influence of machining parameters on the machining performance and associated geometric errors. It is shown that the fuzzy model is capable of giving results providing a good correlation between the real and predicted values. The average error of the model was approximately 1.51% for material removal rate, 3.386% for tool wear rate, 2.924% for wear rate, 5.285% for surface roughness, 4.004% for radial overcut, 4.381% for circularity, and 2.937% for cylindricity.

Keywords Electrical discharge machining (EDM) · Machining performance · Geometrical errors · Machining parameters · Fuzzy logic · Prediction

1 Introduction

Electrical discharge machining (EDM) has become one of the most used processes in manufacturing technology; it plays a crucial role in the field of mechanical production, and therefore, it is an open process for making faced with several improvements. Due to the complexity and optimization objectives, a large number of studies and research are oriented towards new technologies in order to increase productivity, improve the quality of machined parts, and minimize costs and times of production.

In the process of machining by electrical discharge, the machining parameters such as current, voltage, and pulse time, as well as the dielectric, the geometry of the electrodes, and the workpieces play a very important role in the choice of machining performance and quality.

To achieve the required machining performance and quality, it is necessary to take into account an optimal selection of the machining parameters. This selection not only guarantees a reduction in costs and production times but also guarantees control of the phenomena accompanying the machining process, which directly affect the machining performance and quality of the machined parts.

In the context of improving the machining performance and quality of parts machined by electrical discharge machining (EDM), research work in this direction has been analyzed in order to propose better solutions and to support existing scientific research work by remedying certain observed shortcomings and proposing alternative solutions that lead to improvements in the performance measurements of the electrical discharge machining process.

A bibliographic synthesis was carried out to study the effect of the different machining parameters on the performance characteristics of electrical discharge machining. The research carried out in the analyzed works mainly relates to the effect of the parameters of electrical discharge machining such as the current, the voltage, the pulse time, ... and how these affect the performance characteristics of machining as MRR, TWR, EWR, Ra, ROC, and electrode material.

S. Dhanabalan et al. [1] studied the effect of different electrode materials on the machining performance characteristics of the titanium alloy. Copper, brass, and aluminum electrodes

✉ Abderrahim Belloufi
  abelloufi@yahoo.fr

1 Département de Génie Mécanique, Faculté des Sciences Appliquées, Université Kasdi Merbah Ouargla, 30000 Ouargla, Algeria

and kerosene as the dielectric fluid were used in this research. They considered current as an input parameter and MRR, EWR, and Ra as an output parameter. It has been found that a higher MRR is achieved by using brass and aluminum electrodes and that the brass electrodes provide high wear, while the aluminum and copper electrodes provide low wear. A. Torres et al. [2] evaluated the effect of machining parameters of the Inconel 600 alloy machined by EDM and tool materials (graphite) on the electrode wear (EW), the rate of material removal (MRR), and the roughness of machined surfaces for different polarities. The results showed that a higher material removal rate is obtained with a negative polarity. While the low value of electrode wear (EW) and low roughness was obtained with positive polarity. H. Fazlollahtabar et al. [3] analyzed the effect of machining parameters on machining performance. They have developed mathematical models based on the interpolation approach which link the parameters: duty cycle, on time and current by the fineness surface, corrosion rate of the electrode, material removal rate. They also used a fuzzy adaptive neural network to optimize and predict machining performance. Rahul et al. [4] have studied the machinability of four different qualities of Inconel superalloy; they have examined the influence of the variation of interval voltage, peak discharge current, pulse duration, duty cycle, and flushing pressure of the dielectric circulation on the material removal rate, the electrode wear rate; surface roughness and density of surface crack machined by EDM. They showed that increasing the peak current resulted in an improvement in the MRR for different grades of Inconel with an increase in Ra. M. Hanif et al. [5] have studied the influence of the dielectric type, the polarity of the electrodes, the discharge current, and the spark/discharge difference on the material removal rate (MRR) and the surface roughness (Ra) for machining AISI D2 steel. Their results revealed that the kerosene oil and the polarity of the positive led to optimal machining. MK. Pradhan et al. [6] used a neuro-fuzzy model for predicting the material removal rate (MRR), electrode wear, and radial overcut when machining AISI D2 steel. They showed that the discharge current has a very important influence on the material removal rate and the radial overcut. On the other hand, the electrode wear rate is very influenced by the pulse duration. A A. Khan [7] found that when machining aluminum and mild steels with copper and brass electrodes, an increased wear was produced on the electrodes as the discharge current increased. The material removal rate (MRR) also increased with the discharge current. Y. Shen et al. [8] analyzed the effect of peak current, pulse interval, pulse duration on the material removal rate (MRR), and energy consumption during the machining of the titanium alloy Ti-6Al-4V by EDM. They concluded that the most important factor affecting both MRR and energy consumption is current. P. Ong et al. [9] have studied the effect of the machining parameters: the peak current, the pulse interval and the pulse

duration on the material removal rate (MRR) and the electrode wear rate (EWR). They found that an increase in the pulse interval will lead to a reduction in MRR, and that an increase in pulse duration is accompanied by an increase in electrode wear rate (EWR). They also developed a new optimization algorithm to find the optimum machining conditions. T.R. Newton et al. [10] examined the influence of EDM process parameters on the formation of the recoat layer on Inconel 718 samples. They concluded that the average thickness of the recoat layer increased with current discharge, peak, and pulse duration. S.A.K. Rajesha et al. [11] have experimentally studied the effects of variables in the EDM process: pulse current, sensitivity, utilization factor, dielectric rinse pressure, and gap control) on the EDM surface recoat layers splashed. It was concluded that the duty factor and the pulse current influenced the propagation of the cracks. J.H. Zhang et al. [12] proposed an empirical model, built both on the peak current and on the pulse duration, for the electrical discharge machining of ceramics. They concluded that the discharge current had a significant effect on the material removal rate (MRR), while the pulse time had a significant influence on the white layer. M. Kiyak et al. [13] found that with a high current and high pulse time, a high surface finish could be produced, but with a low material removal rate (MRR). They also found that with a high pulse time, a high pulse current, and a low pulse time, you get a high MRR, but with a poor surface finish. HT. Lee et al. [14] noted that the value of the MRR and the surface roughness increased with increasing pulsed current values, but that after certain values, the MRR and the surface roughness decreased due to the expansion of the electric plasma. The pulse current affects the surface crack density; however, the pulse duration influences the degree of crack opening. J.C Rebelo et al. [15]

Fig. 1 Sinking EDM machine ONA NX4

Table 1 Chemical composition of AISI 1095 steel

Element	Content (%)
C	0.95–1.05
Mn	0.15–0.30
Si	0.15–0.30
P	≤ 0.03
S	≤ 0.02
Cr	≤ 0.025
Ni	≤ 0.2
Cu	≤ 0.2

presented an experimental study on the effect of electrical discharge machining parameters on the material removal rate (MRR) and surface quality (Ra) during the machining of copper alloys/high resistance beryllium. The treatment parameters for rough, finishing and micro-finishing, or polishing regimes were analyzed. S. Raj et al. [16] evaluated the effect of different parameters on the machining of EN 45 steel with a copper electrode. The input parameters were peak current (Ip), pulse on time (Ton), pulse off time (Toff), and voltage (V). Pulse on time and current are highly significant parameters, while pulse off time is a less important factor for the material removal rate (MRR). Vikas et al. [17] studied various parameters of the electrical discharge machining process on the surface roughness of the EN41 material. The parameters studied were the peak current (Ip), pulse on time (Ton), pulse off time (Toff), and the voltage (V). They concluded that the discharge current had a greater impact on the roughness of the machined surfaces and that the effect of the other parameters was less significant and can be ignored. Ay et al. [18] studied the influence of electrical discharge machining parameters: the discharge current and the pulse duration on the machining performance of the nickel-based Inconel 718 Super Alloy. They found that the discharge current was more effective on performance than the pulse duration. S. Singh [19] used the Taguchi method and gray relational analysis to analyze the influence of pulse current, pulse duration, duty cycle, and interval voltage

on MRR, tool wear rate, and surface roughness. They came to the conclusion that among all the process parameters, the pulse current showed the strongest effect on all performance. YF. Chen et al. [20] investigated the effect of peak current and pulse duration on MRR, electrode wear rate and surface roughness. They found that the two parameters significantly affected the MRR and the surface roughness. KT. Chiang [21] carried out a survey to study the effect of the parameters: discharge current, pulse time, utilization factor, and open discharge voltage on the variation of MRR, electrode wear rate, and surface roughness. They found that the discharge current and the service factor were the important factors affecting the MRR. YF. Tzeng et al. [22] studied the influence of the EDM process parameters (circuit voltage, pulse duration, duty cycle, pulsed peak current) on surface roughness and geometric precision with the Tagauchi method. They optimized the geometric variation of the machined product by around 28%. Y. Keskin et al. [23] studied the influence of machining parameters: power, pulse time, and spark time on the quality of surfaces machined from steel by EDM. They showed that surface roughness increasing with an increase in discharge duration. SN grigor'ev et al. [24] analyzed the effect of breakdown voltage, peak current, voltage gain, and working voltage on the precision parameters of small diameter holes machined by EDM on oxide carbide ceramic. They concluded that the increase in breakdown voltage, peak current, voltage gain, and working voltage causes changes in the hole diameter. V. Muthukumar et al. [25] predicted the radial overcut by the response surface method according to the machining parameters: the current, pulse on time, pulse off time, and voltage. It was concluded that current and voltage have a significant effect on the radial overcut.

From the literature search presented above, it can be concluded that there is a great need for the development of more precise methods for measuring the performance of electrical discharge machining (EDM) as well as the errors related to the machined shapes. It is also clear that the construction of models for predicting the electrical discharge machining
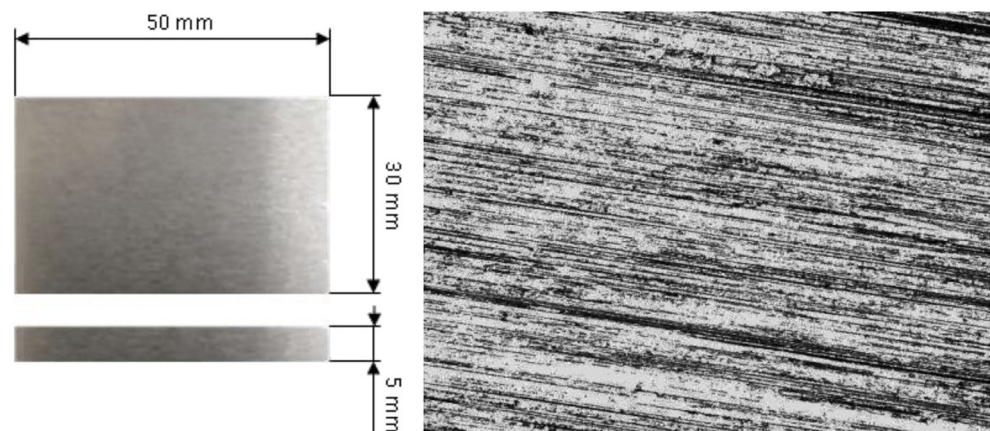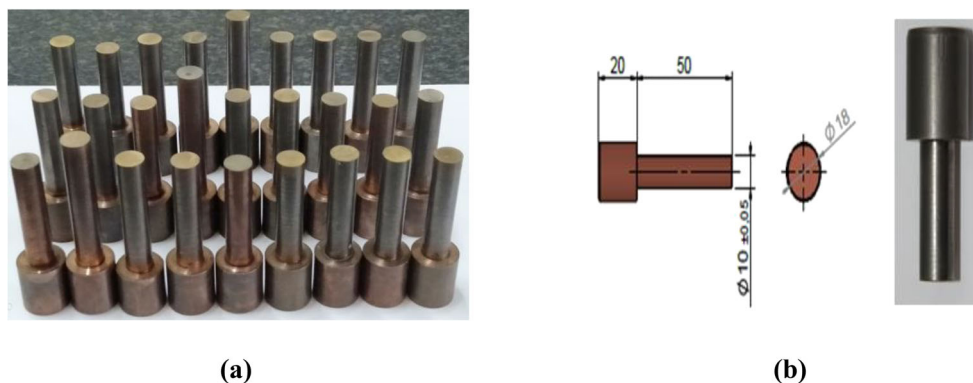
Fig. 2 Workpiece

Fig. 3 Electrodes used in the tests

(a) (b)

performance depends not only on the method used for the construction of the models but also on the experimental procedure followed. Most scientific research on this subject uses data from the literature, which requires more experimental development to measure machining performance.

In most of the work carried out, two or three machining performances have been considered as outputs of the prediction system. In addition, little scientific research has already tackled the problem of geometric errors associated with electrical discharge machining.

This is why, in this paper, on the basis of experimental measurement tests of the electrical discharge machining performance and the geometric errors associated with the machining of the holes, the effects of the machining parameters, on these performances, and these errors are predicted with an intelligent method based on a fuzzy multi-output inference system. The prediction results found by this model have been approved by other experimental tests.

2 Experimental procedure

2.1 Materials and equipment

All tests were carried out under industrial conditions using an ONA NX4 machine tool (13.7 KVA connected load, working table dimension 800×600 mm, maximum working height 400 mm) which is a Sinking EDM machine as shown in Fig. 1.

The tests were carried out by machining prismatic parts of AISI 1095 treated steel.

AISI 1095 is specially designed for the manufacture of molds, tools, impression plates, punches and dies; they are also used in the manufacture of finished or semi-finished parts which require wear resistance high.

The chemical composition of AISI 1095 steel is described in Table 1.

The workpieces used in this study delivered in the standardized state allows after thermal tempering to obtain a significant surface hardness (60 to 65 HRC) and were prepared for the size of $50 \times 30 \times 5$ mm ± 0.2 as shown in Fig. 2 and the upper surface has been highly finished to obtain a real flatness; the density of the materials is 7.78 g/cm^3.

Surface roughness measurements were made after the finishing process of each part to ensure that the part was ready for testing. The roughness of the surface found on all the parts varied between 0.1 and 0.17 μm.

The electrodes used in this study are cupro-tungsten electrodes (Fig. 3a): an alloy made from the powder metallurgy process, with 40% copper (Cu), with a grain size < 150 (μ) and 60% tungsten (W) has an average grain size between 20 (μ) and 100 (μ). This alloy has unique physical properties. One of the most important benefits of tungsten is high-temperature resistance, while copper increases thermal and electrical conductivity.

The electrodes were machined so as to obtain a length of 50 mm and a diameter of the working part 10 ± 0.05 mm (Fig. 3b). The base surface and the side surface of the electrode were highly finished, using abrasive paper, to obtain a fine surface.

The properties of the tungsten copper electrodes used in the tests are given in Table 2.

Table 2 Properties of electrodes

Electrodes	Density (g/cm3)	Hardness (HB ≥)	Electrical resistivity	Electrical conductivity (IACS % ≥)
Cu40W60	12.75	140	3.7	47

Fig. 4 Three-dimensional measuring machines 443 Dual Z

For the measurement of the circularity and the cylindricity of the machined holes, a coordinate measuring machine, OPTIV Performance 443 Dual Z (MMT) manufactured by HEXAGON METROLOGY SAS, was used. This machine combines optical and tactile measurement in a single system; it supports multi-sensor measurements using the vision sensor, the touch trigger, and the scanning probe (Fig. 4).

Voyager Pro digital density meter Model: VP6102 C (Fig. 5) is used to measure the density of electrodes and workpieces.

The workpieces and the electrode were weighed before and after the machining of each experiment on an AP 250 D balance (Fig. 6) with precision 0.0001 g to determine the weight loss. These values were then used to calculate the material removal rate and the tool wear rate.

For surface measurement a roughness meter (Mitutoyo-sufftest-211), shown in Fig. 7 is used. It consists of a stylus that moves mechanically over a surface to record the roughness of the surface over a determined sample length.

Fig. 5 Voyager Pro digital density meter Model: VP6102 C

Fig. 6 AP 250 D balance

2.2 Experimental setup

Twenty-seven (27) tests were carried out using three input (control) parameters; each of these parameters varies to three discrete level values as illustrated in Table 3. These parameters are current (I), voltage (V), and pulse on time (Ton).

There are many machining parameters that affect the electrical discharge machining performance. Current, voltage, and pulse on time are the most active influence parameters on machining performance. Advantageously, these parameters are also the easiest to adjust, and can directly modify their value in EDM machine with no additional cost. Thus, other important parameters were not considered (such as pulse off time, polarity, gap) whose values were kept throughout experiments. The constant parameters and corresponding values were pulse off time = 50 μs; polarity: direct; gap = 0.5 mm; fluid pressure = 16 kg/cm^2).

The tests concern the production of 3.5-mm-deep holes. On each part, three holes were made with variation of the three control parameters according to the experiment plans chosen (Fig. 8). Each test ends when the electrode reaches a depth of 3.5 mm.

In addition to this, another series of tests (seven tests) was carried out with the same experimental conditions but with other input parameters. The results of these tests were later used to validate the models built.

Fig. 7 Roughness meter (Mitutoyo-sufftest-211)

Table 3 Settings of process control parameters

Parameters	Unit	Levels		
		P	M	G
Current (I)	A	12	14	16
Voltage (V)	V	120	160	200
Pulse on time (Ton)	µs	100	200	400

A view of all the parts machined during the twenty-seven (27) tests carried out was provided in Fig. 9.

It is important to note that in order to improve the reliability of the measurements, the points below are taken into account:
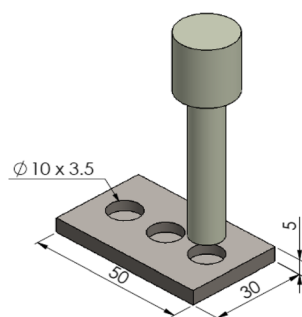
1. All measurements are carried out in a fully closed controlled room at a temperature of 20 ± 1 °C and the humidity is $50 \pm 5\%$.
2. Each part has been thoroughly cleaned with acetone before measurement.
3. Measurements are performed in a short time by a single operator using the same equipment.
4. Ensure the fidelity of measuring instruments and devices: the calibration of the measuring instruments and devices was carried out before each test.

    The three-dimensional measuring machine 443 Dual Z is calibrated according to normative reference: ISO 10360-2.

    The digital micrometer is calibrated according to the normative reference: ISO 3611.

    The roughness meter (Mitutoyo-sufftest-211) is calibrated according to the normative reference: ISO 5436.
5. Ensure the measurement trueness: each measure was conducted three times and the average of the obtained results was considered. Standard deviation of the three readings after each of the 27 experiments was calculated and the reliability coefficient is determined.

Fig. 9 Workpieces used in the tests after machining

2.2.1 Determination of the material removal rate

The average weight of material removed from the workpiece per unit of time during machining is called the material removal rate. It directly determines the machining efficiency of the process. It is generally measured in mm³/min. Mathematically, it can be expressed as
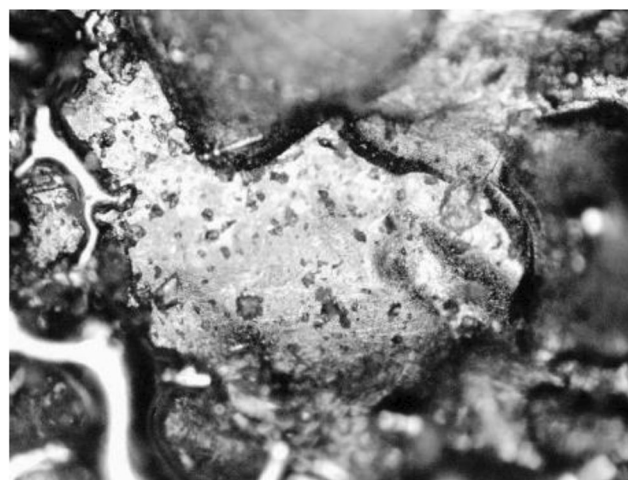

Fig. 8 The machining configuration of workpiece

Fig. 10 Microscopic visualization of the machined surface

Fig. 11 Measure of circularity

Video camera system

Pc-dmis software
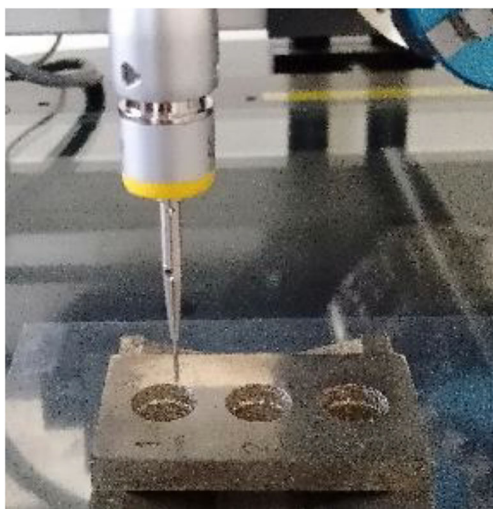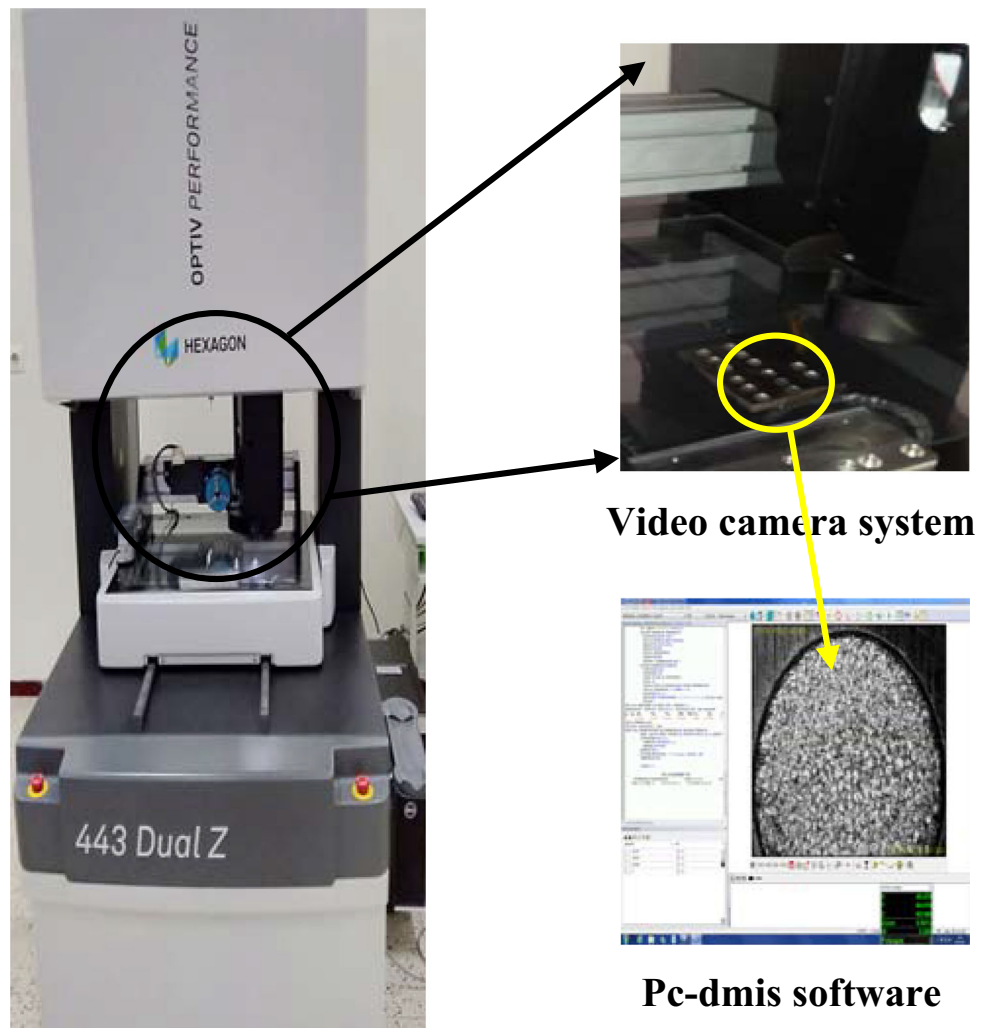
$$MRR = \frac{1000\Delta W_W}{\rho_W T} \qquad (1)$$

ΔW_W is the weight loss of the working material during machining;

ρ_W is the density of the workpiece material;

T is the machining time.

2.2.2 Determination of the tool wear rate (EWR)

The average weight of the material lost of the tool per unit of time during machining is called the tool wear rate (TWR). It is directly linked to the precision and profitability of the machining. The tool life plays an important role in increasing productivity. It is expressed by this equation:
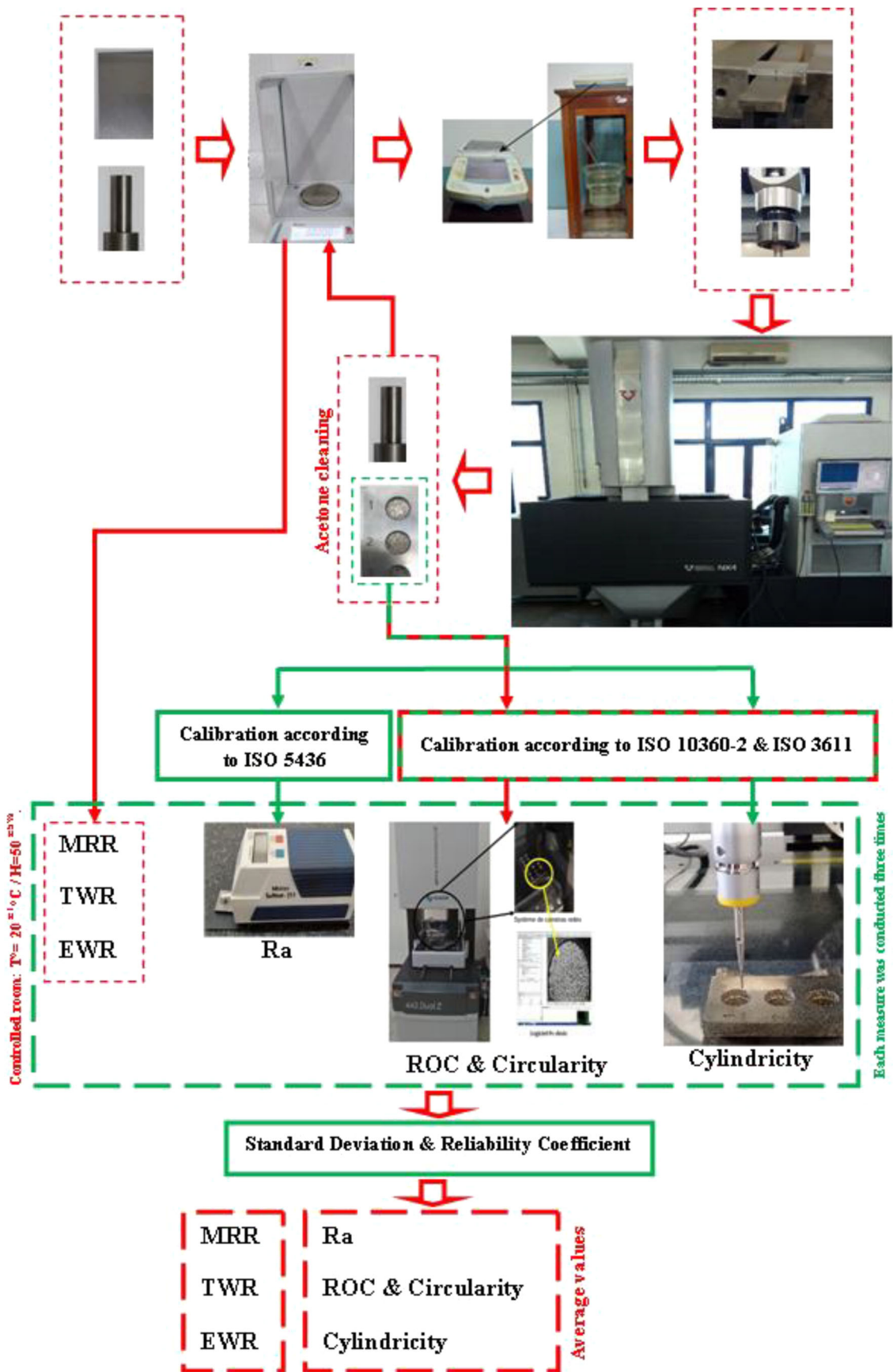

Fig. 12 Measure of cylindricity

Fig. 13 Experimental setup

Table 4 Experimental conditions and results

Test	I (A)	V (V)	Ton (μs)	MRR (mm³/min)	TWR (mm³/min)	WR (%)	Ra (μm)	ROC (mm)	CIR (mm)	CYL (mm)
1	12	120	100	51.48	1.97	3.83	1.45	0.162	0.031	0.0233
2	14	120	100	45.87	2.02	4.40	3.39	0.171	0.0329	0.0258
3	16	120	100	53.83	1.59	2.96	6.05	0.161	0.0388	0.0468
4	12	120	200	48.35	1.74	3.59	1.03	0.211	0.0606	0.0686
5	14	120	200	44.82	1.75	3.90	1.18	0.218	0.0575	0.0389
6	16	120	200	45.65	1.93	4.23	1.72	0.207	0.0418	0.0284
7	12	120	400	49.46	2.03	4.11	0.7	0.238	0.0505	0.0703
8	14	120	400	48.52	1.80	3.71	3.27	0.227	0.0592	0.0684
9	16	120	400	55.24	2.02	3.65	1.3	0.251	0.068	0.0628
10	12	160	100	47.03	1.68	3.57	3.05	0.186	0.0462	0.0483
11	14	160	100	39.56	1.31	3.31	3.81	0.189	0.047	0.0395
12	16	160	100	43.61	1.55	3.56	6.42	0.172	0.0458	0.03
13	12	160	200	47.85	1.82	3.20	1.78	0.221	0.0479	0.0493
14	14	160	200	48.44	1.46	3.02	0.46	0.198	0.0329	0.0631
15	16	160	200	48.23	1.25	2.59	2.05	0.241	0.0446	0.0684
16	12	160	400	59.81	1.53	2.01	2.59	0.26	0.0499	0.0696
17	14	160	400	55.93	1.65	2.94	1.88	0.258	0.0416	0.0679
18	16	160	400	55.03	1.33	2.41	6.62	0.256	0.0468	0.0532
19	12	200	100	54.43	1.34	2.46	3.96	0.176	0.067	0.04
20	14	200	100	48.07	0.95	1.97	2.56	0.177	0.0453	0.0316
21	16	200	100	46.75	1.45	3.11	5.06	0.156	0.0371	0.0667
22	12	200	200	57.01	1.76	3.09	6.59	0.219	0.0472	0.0462
23	14	200	200	56.28	1.59	2.82	1.38	0.226	0.0534	0.062
24	16	200	200	59.95	1.09	1.82	2.28	0.24	0.0513	0.0553
25	12	200	400	59.49	1.53	2.57	3.16	0.233	0.0558	0.052
26	14	200	400	52.95	1.22	2.31	1.64	0.248	0.0439	0.0654
27	16	200	400	57.70	1.54	2.67	2.34	0.248	0.0465	0.0436

$$TWR = \frac{1000\Delta W_T}{\rho_T T} \qquad (2)$$

ΔW_T is the weight loss of the electrode material during machining;

ρ_T is the density of the electrode material;

2.2.3 Determination of the wear rate

The wear rate is defined as the ratio between the tool removal rate and the material removal rate. It is usually expressed as a percentage as shown in Eq. (3)

$$WR = \frac{100TWR}{MRR} \qquad (3)$$

Fig. 14 Fuzzy system

[12 12 14]   L
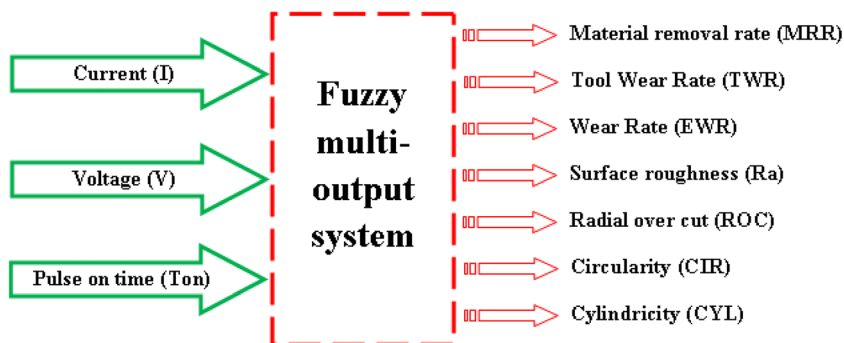[12 14 16]   M
[14 16 16]   H

Fig. 15 Linguistic variables for current (I)

2.2.4 Surface roughness measurement

In EDM, the fatigue strength of the machined component is strongly influenced by the quality of the machined surface. The quality of the machined surface strongly depends on the energy per spark and the size of the craters. Figure 10 illustrates the surface machined during a test among the twenty-seven tests carried out.

Surface roughness measurement was taken at 3 different locations, and average values are reported, where cutoff length is kept at 0.8 during the surface roughness measurement. Standard deviation of the three roughness readings varies between 0.082 and 0.93, and the reliability coefficient (Cronbach's alpha) is around 0.976.

2.2.5 Radial overcut

The radial overcut is expressed as the difference in the radius of the hole produced compared to the radius of the electrode used. It is given by Eq. (4)

$$ROC = \frac{(D_h - D_T)}{2} \tag{3}$$

D_h is the diameter of the hole.
D_T is the diameter of the tool.

The diameter of the holes was measured three times, using the three-dimensional measuring machine 443 Dual Z, and the average of the results obtained was considered. Standard deviation of the three measures varies between 0.002 and 0.007, and the reliability coefficient (Cronbach's alpha) is around 0.9984. A negligible variation is noted when measuring the diameter of the electrodes.

2.2.6 Measure of circularity

The circularity is considered as a difference between the radial distances from the nearest point and the furthest from the geometric center of the hole.

[120 120 160]   L
[120 160 200]   M
[120 200 200]   H

Fig. 16 Linguistic variables for voltage (V)

[100 100 200]   L
[100 200 400]   M
[200 400 400]   H

Fig. 17 Linguistic variables for pulse on time (Ton)

To produce the desired tolerance, the electrical discharge machining process faces a challenge to produce zero circularity; this is due to debris exiting the hole with the dielectric fluid under pressure, which causes wear on the upper part of the hole.

In this work, the circularity is measured using the automatic element estimation mode on the PC-DMIS Vision software which controls the three-dimensional measuring machine 443 Dual Z (Fig. 11).

The circularity was measured three times and the average of the results obtained was considered. Standard deviation of the three measures varies between 0.0003 and 0.004, and the reliability coefficient (Cronbach's alpha) is around 0.9939.

2.2.7 Measure of cylindricity

Cylindricity defines the shape deviation of a cylinder. Their tolerance defines a band between two concentric cylinders in which the real shape of the cylinder to which the tolerance must apply.

In this work, the cylindricity measured using the cylinder measurement option in the PC-DMIS software which controls the three-dimensional measuring machine (Fig. 12).

The cylindricity was measured three times and the average of the results obtained was considered. Standard deviation of the three measures varies between 0.0003 and 0.002, and the reliability coefficient (Cronbach's alpha) is around 0.9994.

The configuration of the experimental setup is presented in Fig. 13.
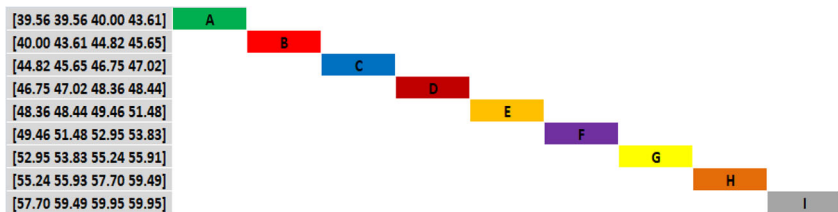
The study of the variation of various performance measures as a function of the parameters leads to finding the values of these parameters mentioned in Table 4.

3 Fuzzy models

In this work, the fuzzy model designed to predict various performance measures for electrical discharge machining uses three inputs and seven outputs (Fig. 14). Current (I), voltage (Volt), and pulse on time (Ton) are the inputs and the cutting electrical machining discharge performance is the output of the system.

The first step in the study of the performance measures for electrical discharge machining algorithm is to choose the forms of the membership functions for the process variables according to the experimental database, which were used on the machine tool. Fuzzy expressions for current (I), voltage (V), and pulse on time (Ton) and performances measures for

Fig. 18 Linguistic variables for material removal rate (MRR)

Interval
[39.56 39.56 40.00 43.61]
[40.00 43.61 44.82 45.65]
[44.82 45.65 46.75 47.02]
[46.75 47.02 48.36 48.44]
[48.36 48.44 49.46 51.48]
[49.46 51.48 52.95 53.83]
[52.95 53.83 55.24 55.91]
[55.24 55.93 57.70 59.49]
[57.70 59.49 59.95 59.95]

electrical discharge machining: material removal rate (MRR), tool wear rate (TWR), wear rate (WR), surface roughness (Ra), radial overcut (ROC), circularity (CIR), and cylindricity (CYL) are shown in Figs. 15, 16, 17, 18, 19, 20, 21, 22, 23, and 24, respectively.

3.1 Fuzzy expressions

The numerical values of current (I) are linked by linguistic variables as shown in Fig. 15.

The numerical values of voltage (V) are linked by linguistic variables as shown in Fig. 16.

Numerical pulses on time (Ton) values are linked by linguistic variables as shown in Fig. 17.

The numerical values of material removal rate (MRR) are linked by linguistic variables as shown in Fig. 18.

The numerical values of tool wear rate (TWR) are linked by linguistic variables as shown in Fig. 19.

The numerical values of the electrode wear rate (WR) are linked by linguistic variables as shown in Fig. 20.

The numerical values of surface roughness (Ra) are linked by linguistic variables as shown in Fig. 21.

The numerical values of radial overcut (ROC) are linked by linguistic variables as shown in Fig. 22.

The numerical values of circularity (CIR) are linked by linguistic variables as shown in Fig. 23.

The numerical values of cylindricity (CYL) are linked by linguistic variables as shown in Fig. 24.

Membership functions come in many forms. In this study, triangular membership functions for the input variables and trapezoidal for the output parameters were used for the construction of the first model.

The choice of this type of membership function is due to the nature of the experimental data; it is noted that the values of the input parameters are limited (each parameter is determined by three values). The triangular membership functions are suitable for this type of data and it suffices to determine the central value and the slope of each side.

On the other hand, the output seems more complicated because it is represented by several values; these values are divided into intervals. These intervals are represented by trapezoidal shapes.

For the second model, the Gaussian membership functions for the input variables and the PIMF membership functions for the output parameters were used.

The triangular membership functions for the input and the trapezoidal membership functions for output parameters of the first model are illustrated in Fig. 25.

The Gaussian membership functions for the input and the PIMF membership functions for output parameters of the second model are illustrated in Fig. 26.

3.2 Fuzzy rules

The fuzzy model was created from twenty-seven (27) fuzzy rules defined on the basis of experimental work (the twenty-seven tests carried out).

The fuzzy system created has three input parameters to produce seven outputs; the fuzzy rules can be described in matrix form. Table 5 shows the set of matrix rules between input parameters and output performances.

The second column indicates the fuzzy sets for current (P: low current, M: medium current, G: high current) from low current to high current. The third column indicates the fuzzy sets for voltage varying from low voltage to high voltage (P: low voltage, M: average voltage, G: high voltage), the fourth column indicates the fuzzy sets for Pulse on time varying from low pulse on time to high pulse on time (TP: low pulse on time, M: average pulse on time G:

Fig. 19 Linguistic variables for wear rate (TWR)

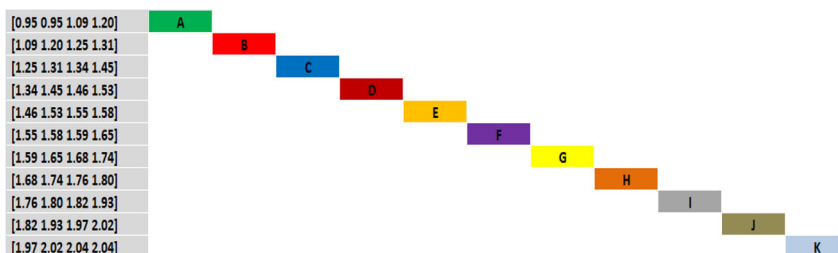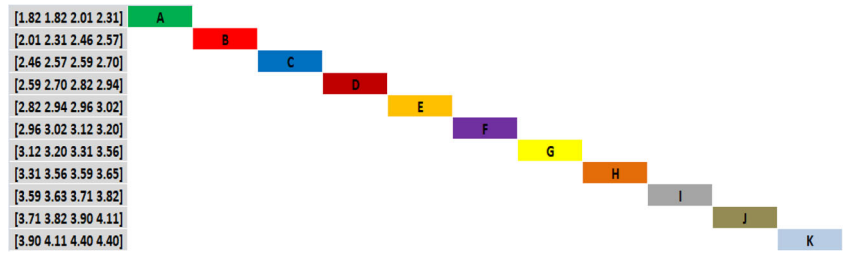| Interval |
|---|
| [0.95 0.95 1.09 1.20] |
| [1.09 1.20 1.25 1.31] |
| [1.25 1.31 1.34 1.45] |
| [1.34 1.45 1.46 1.53] |
| [1.46 1.53 1.55 1.58] |
| [1.55 1.58 1.59 1.65] |
| [1.59 1.65 1.68 1.74] |
| [1.68 1.74 1.76 1.80] |
| [1.76 1.80 1.82 1.93] |
| [1.82 1.93 1.97 2.02] |
| [1.97 2.02 2.04 2.04] |

Fig. 20 Linguistic variables for electrode wear rate (WR)

high pulse on time). Contents of the matrix are the result obtained, which is the outputs for this study. The fuzzy operators used in the rules will apply are: "and", "or." Some examples of fuzzy rules in linguistic form are presented below:
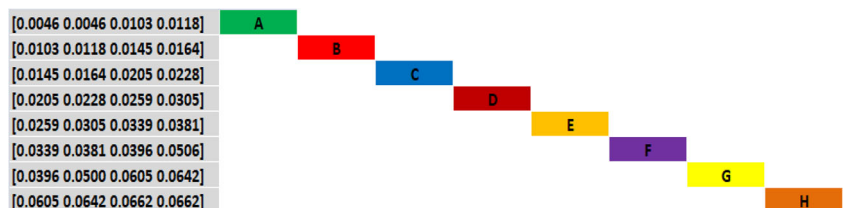
> 1. If I is (P: low) and V is (P: low) and Ton is (P: low) Then: MMR is (F) and TWR is (J) and WR is (J) and Ra is (B) and ROC is (A) and CIR is (A) and CYL is (A)
> 2. If I is (M: average) and V is (P: low) and Ton is (P: low) Then: MMR is (C) and TWR is (K) and WR is (K) and Ra is (E) and ROC is (B) and CIR is (A) and CYL is (A)
> 3. If I is (G: high) and V is (P: low) and Ton is (P: low) Then: MMR is (G) and TWR is (F) and WR is (E) and Ra is (H) and ROC is (A) and CIR is (B) and CYL is (D)

> 27. If I is (G: high) and V is (G: high) and Ton is (G: high) Then: MMR is (H) and TWR is (E) and WR is (D) and Ra is (D) and ROC is (G) and CIR is (D) and CYL is (D)

3.3 Defuzzification and study of the error and accuracy of fuzzy models

The constructed model uses a continuous universe for all the input and output variables. So the input can be any combination of three variables (current, voltage and pulse on time) and the outputs are: material removal rate (MRR), tool wear rate (TWR), wear rate (WR), surface roughness (Ra), radial overcut (ROC), circularity (CIR), and cylindricity (CYL). Defuzzification makes it possible to merge the different rules generated by the inference engine to give it only one value of each output and to transform this linguistic output variable

into digital data by calculating the abscissa of the center of gravity of the membership function.

Seven new tests that are not entered into the model creation process were carried out. It will be used to verify the model. These tests were carried out under the same conditions as the previous tests, but with different machining parameters.

To calculate the error percentage of the seven tests, we use Eq. (4):

$$e_i = \left[\frac{\left| Output_{exp} - Output_{pred} \right|}{Output_{exp}} \right] \times 100 \qquad (4)$$

To calculate the percentage of the accuracy of the 7 tests, Formula (5) is used:

$$A = \frac{1}{N} \sum_{i=1}^{N} \left[1 - \frac{\left| Output_{exp} - Output_{pred} \right|}{Output_{exp}} \right] \times 100 \qquad (5)$$

4 Results

Table 6 groups the values of the outputs obtained with the two fuzzy logic models in terms of the maximum, minimum, standard deviation, and coefficient of variation, the accuracy, and the error rate for the seven new tests are also presented in this table.

The difference in the precision of the two models shows that it is possible to use either of them with little preference for the first model.

4.1 Result of material removal rate

The results of defuzzification of the first output (MRR) are shown in Fig. 27.
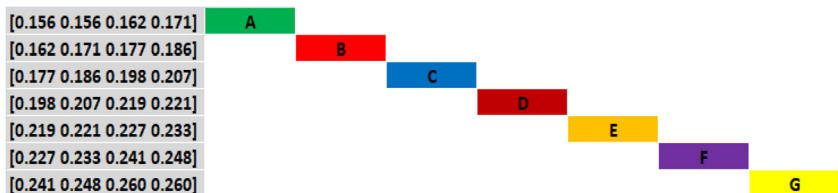
Fig. 21 Linguistic variables for surface roughness (Ra)

Fig. 22 Linguistic variables for radial overcut (ROC)

[0.156 0.156 0.162 0.171]
[0.162 0.171 0.177 0.186]
[0.177 0.186 0.198 0.207]
[0.198 0.207 0.219 0.221]
[0.219 0.221 0.227 0.233]
[0.227 0.233 0.241 0.248]
[0.241 0.248 0.260 0.260]

Fig. 23 Linguistic variables for circularity (CIR)

[0.0310 0.0310 0.0329 0.0371]
[0.0329 0.0371 0.0388 0.0416]
[0.0388 0.0416 0.0439 0.0446]
[0.0439 0.0446 0.0479 0.0499]
[0.0479 0.0499 0.0534 0.0558]
[0.0534 0.0558 0.0575 0.0592]
[0.0575 0.0592 0.0606 0.0670]
[0.0606 0.0670 0.0680 0.0680]
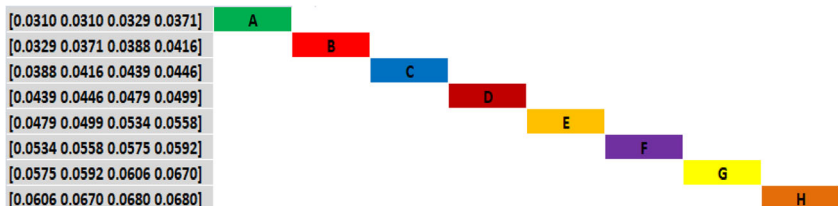
Figure 28 shows the capacity of the fuzzy model constructed to predict the material removal rate (MRR). For the same machining parameters, the material removal rate obtained by the fuzzy model and the confirmation tests are shown in Fig. 28.

The results of the confirmatory tests have shown that the fuzzy model constructed gives values of the material removal rate (MRR) close to the real values. The maximum and minimum deviation of the predicted material removal rate (MRR) and the real material removal rate (MRR) is observed at 0.084 mm^3/min and 1.544 mm^3/min, respectively. The predicted accuracy of the fuzzy model constructed is 98.489%.

4.2 Result of tool wear rate

The results of defuzzification of the second output (TWR) are shown in Fig. 29.

Figure 30 shows the ability of the fuzzy model constructed to predict the tool wear rate (TWR). For the same machining parameters, the tool wear rate obtained by the fuzzy model and the confirmation tests are shown in Fig. 30.

The results of the confirmation tests have shown that the fuzzy model constructed gives tool wear rate (TWR) values close to the real values. The maximum and minimum deviation of the predicted tool wear rate (TWR) values with the real tool wear rate (TWR) is observed at 0.01 mm^3/min and 0.099 mm^3/min, respectively. The

prediction accuracy of the fuzzy model constructed is 96.614%.

4.3 Result of wear rate

The results of defuzzification of the third output (WR) are shown in Fig. 31.

Figure 32 shows the ability of the fuzzy model constructed to predict the wear rate (WR). For the same machining parameters, the wear rate (WR) obtained by the fuzzy model and the confirmation tests are shown in Fig. 32.

The results of the confirmation tests have shown that the fuzzy model constructed gives values of the wear rate (WR) close to the real values. The maximum and minimum deviation of the wear rate (WR) values predicted with the real wear rate (WR) is observed at 0.004% and 0.205%, respectively. The prediction accuracy of the fuzzy model constructed is 97.076%.

4.4 Result of surface roughness

The results of defuzzification of the fourth output (Ra) are shown in Fig. 33.

Figure 34 shows the ability of the fuzzy model constructed to predict the surface roughness (Ra). For the same machining parameters, the surface roughness (Ra) obtained by the fuzzy model and the confirmation tests are shown in Fig. 34.
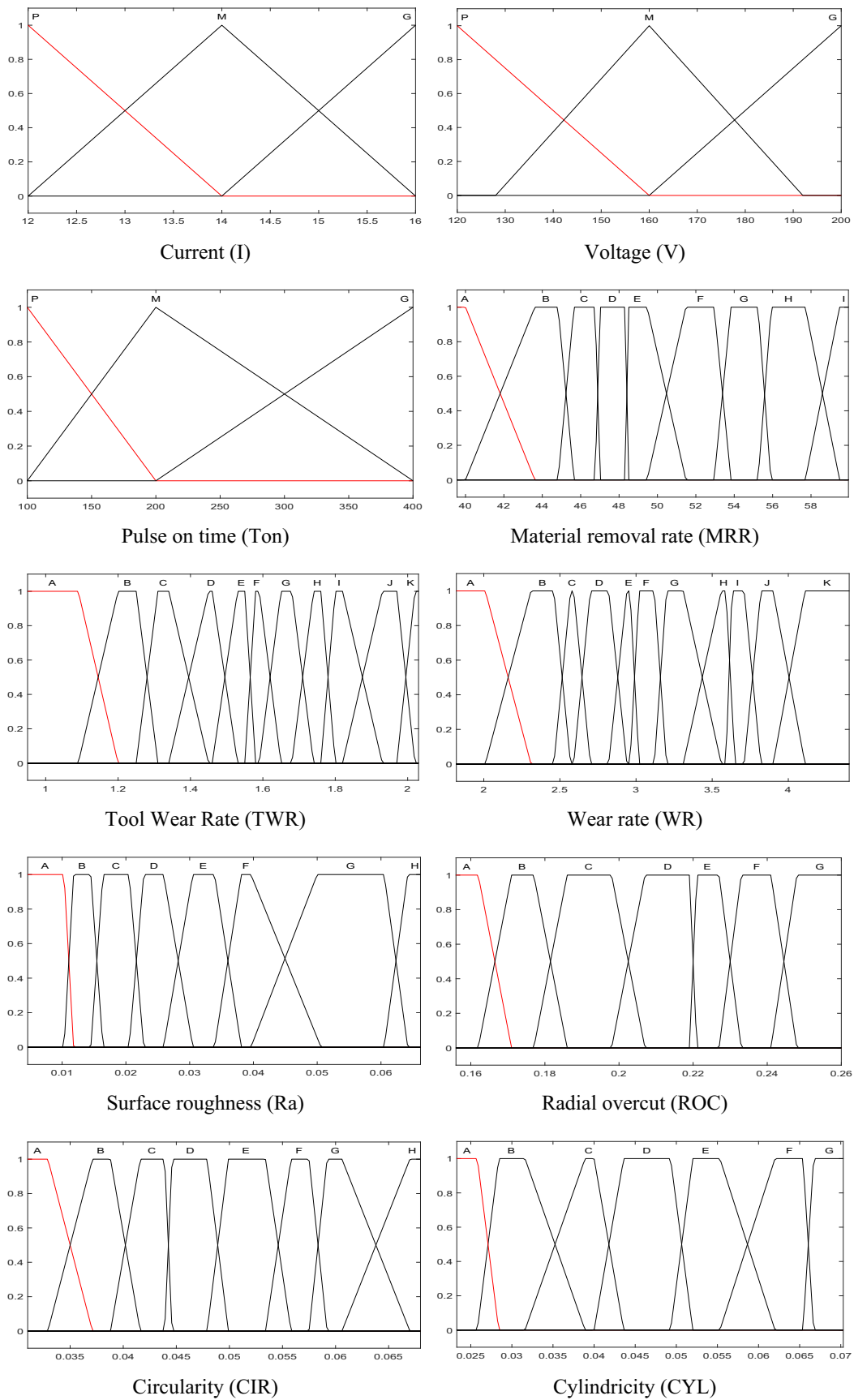
Fig. 24 Linguistic variables for cylindricity (CYL)

[0.0233 0.0233 0.0258 0.0284]
[0.0258 0.0284 0.0316 0.0389]
[0.0316 0.0389 0.0400 0.0436]
[0.0400 0.0436 0.0493 0.0520]
[0.0493 0.0520 0.0553 0.0620]
[0.0553 0.0620 0.0654 0.0667]
[0.0654 0.0667 0.0703 0.0703]

Fig. 25 Membership functions for input and output parameters using triangular and trapezoidal membership
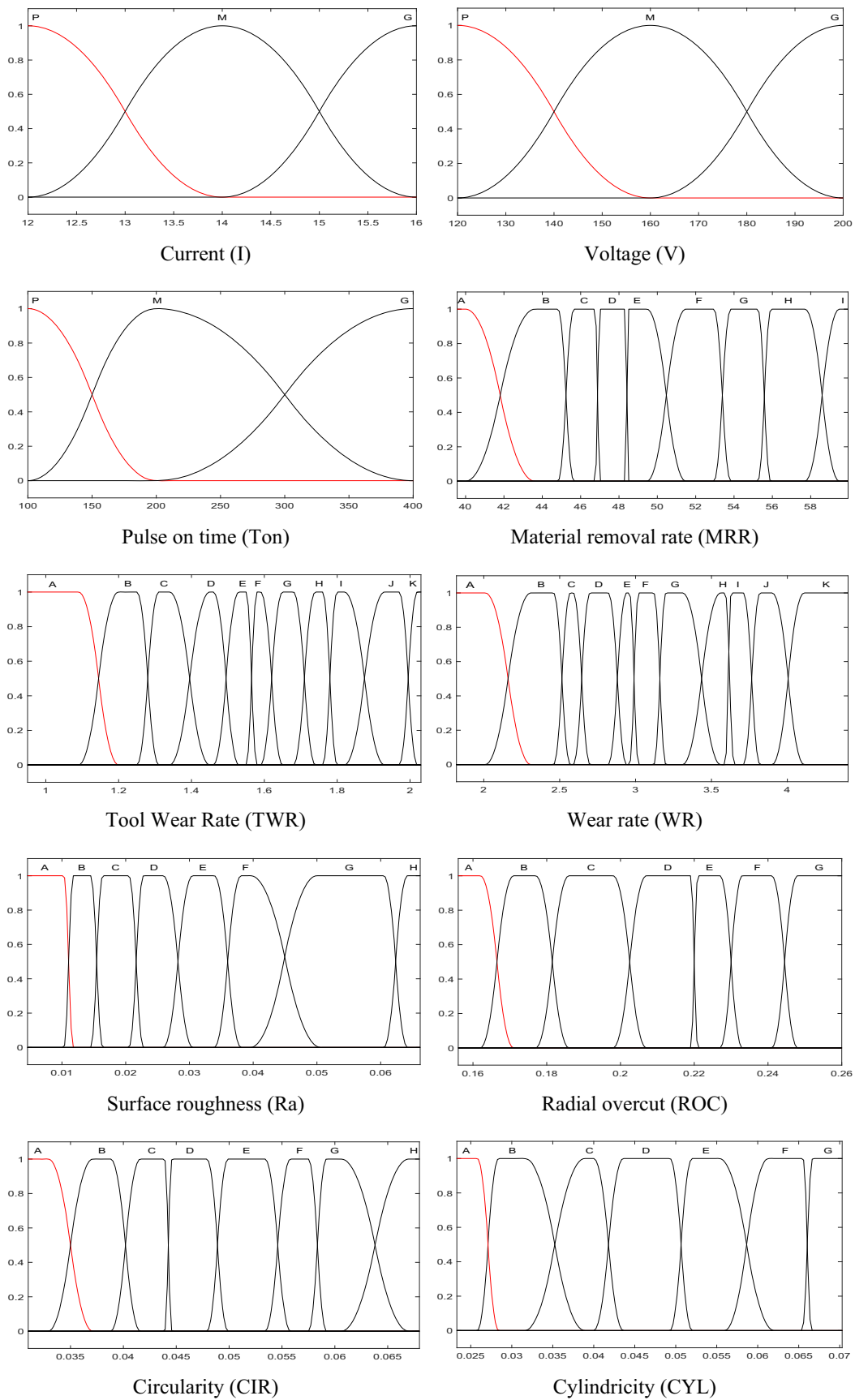
Fig. 26 Membership functions for input and output parameters using Gaussian and Pimf membership

Table 5   Inference table

Test	I (A)	V (V)	Ton (μs)	MRR (mm³/min)	TWR (mm³/min)	WR (%)	Ra (μm)	ROC (mm)	CIR (mm)	CYL (mm)
1	P	P	P	F	J	J	B	A	A	A
2	M	P	P	C	K	K	E	B	A	A
3	G	P	P	G	F	E	H	A	B	D
4	P	P	M	D	H	H	A	D	G	G
5	M	P	M	B	H	J	B	D	F	C
6	G	P	M	C	J	K	C	D	C	B
7	P	P	G	E	K	K	A	F	E	G
8	M	P	G	E	I	I	E	E	G	G
9	G	P	G	G	K	I	B	G	H	F
10	P	M	P	D	G	H	E	C	D	D
11	M	M	P	A	C	G	F	C	D	C
12	G	M	P	B	E	H	H	B	D	B
13	P	M	M	E	E	G	C	E	D	D
14	M	M	M	E	D	F	A	C	A	F
15	G	M	M	D	B	C	C	F	D	G
16	P	M	G	I	B	A	D	G	E	G
17	M	M	G	H	G	E	C	G	C	G
18	G	M	G	G	C	B	H	G	D	E
19	P	G	P	G	C	B	F	B	H	C
20	M	G	P	E	A	A	D	B	D	B
21	G	G	P	C	D	F	G	A	B	G
22	P	G	M	H	H	F	H	D	D	D
23	M	G	M	H	F	D	B	E	E	F
24	G	G	M	I	A	A	D	F	E	E
25	P	G	G	I	E	C	E	F	F	E
26	M	G	G	F	B	B	C	G	C	F
27	G	G	G	H	E	D	D	G	D	D

The results of the confirmation tests have shown that the fuzzy model constructed gives values of surface roughness (Ra) close to the real values. The maximum and minimum deviation of the predicted surface roughness (Ra) values with the real surface roughness (Ra) is observed at 0.5 μm and 0.17 μm, respectively. The predicted accuracy of the fuzzy model constructed is 94.715%.

4.5 Result of radial overcut

The results of defuzzification of the fifth output (ROC) are shown in Fig. 35.

Figure 36 shows the ability of the fuzzy model constructed to predict radial overcut (ROC). For the same machining parameters, the radial overcut (ROC) obtained by the fuzzy model and the confirmation tests are shown in Fig. 36.

The results of the confirmation tests have shown that the fuzzy model constructed gives values of Radial overcut (ROC) close to the real values. The maximum and minimum deviation of the predicted radial overcut (ROC) values with

the real radial overcut (ROC) is observed at 0.0047 mm and 0.017 mm, respectively. The predicted accuracy of the fuzzy model constructed is 95.996%.

4.6 Result of circularity

The results of defuzzification of the sixth output (CIR) are shown in Fig. 37.

Figure 38 shows the ability of the constructed fuzzy model to predict circularity (CIR). For the same machining parameters, the circularity (CIR) obtained by the fuzzy model and the confirmation tests are shown in Fig. 38.

The results of the confirmation tests have shown that the fuzzy model constructed gives circularity (CIR) values close to the real values. The maximum and minimum deviation of the predicted circularity (CIR) values with the real circularity (CIR) is observed at 0.0001 mm and 0.0033 mm, respectively. The prediction precision of the fuzzy model constructed is 95.619%.

Table 6 Fuzzy system error and accuracy for the confirmation tests

Outputs	Model	Output min	Output max	Standard deviation	Coef. of variation	Error %	Accuracy %
MRR (mm^3/min)	Model 1	46.1	57.2	3.642	0.069	1.511	98.489
	Model 2	45.6	57.1	3.762	0.072	1.51	98.49
TWR (mm^3/min)	Model 1	1.26	1.86	0.248	0.164	3.386	96.614
	Model 2	1.25	1.86	0.234	0.153	4.142	95.858
WR (%)	Model 1	2.34	3.84	0.602	0.202	2.924	97.076
	Model 2	2.33	3.79	0.574	0.191	4.861	95.139
Ra (µm)	Model 1	1.01	2.51	0.521	0.301	5.285	94.715
	Model 2	1.00	2.50	0.563	0.339	9.192	90.808
ROC (mm)	Model 1	0.191	0.25	0.024	0.111	4.004	95.996
	Model 2	0.043	0.247	0.068	0.359	4.333	95.667
CIR (mm)	Model 1	0.0366	0.0545	0.006	0.122	4.381	95.619
	Model 2	0.0358	0.0566	0.006	0.140	5.016	94.984
CYL (mm)	Model 1	0.0449	0.0632	0.006	0.119	2.937	97.063
	Model 2	0.0466	0.0632	0.006	0.114	3.139	96.861

4.7 Result of cylindricity

The results of defuzzification of the seventh output (CYL) are shown in Fig. 39.

Figure 40 shows the ability of the fuzzy model constructed to predict cylindricity (CYL). For the same machining parameters, the cylindricity (CYL) obtained by the fuzzy model and the confirmation tests are shown in Fig. 40.

The results of the confirmation tests have shown that the fuzzy model constructed gives values of cylindricity (CYL) close to the real values. The maximum and minimum deviation of the predicted cylindricity (CYL) values with the real cylindricity (CYL) is observed at 0.0001 mm and 0.0033 mm, respectively. The prediction precision of the fuzzy model constructed is 97.063%.

5 Graphical representation of electrical discharge machining performances

5.1 Material removal rate

The influence of the current on the MRR is shown in Fig. 41a and b. It can be observed in these figures that the variation in the current is not significant and remains almost stable. This tendency can be at the interval of the current chosen in this study which has high levels [12, 16]. This tendency has been observed at high current levels, due to excessive and counterproductive discharge. This leads to an increase in the size of the plasma channel over time during discharge, which results in a loss of energy in the dielectric causes a decrease in material removal. The same observation was noted by O. Pauline et al. [9] and F. Klocke et al. [26].

Fig. 27 Variation of the experimental and predicted material removal rate (MRR) as a function of the number of tests
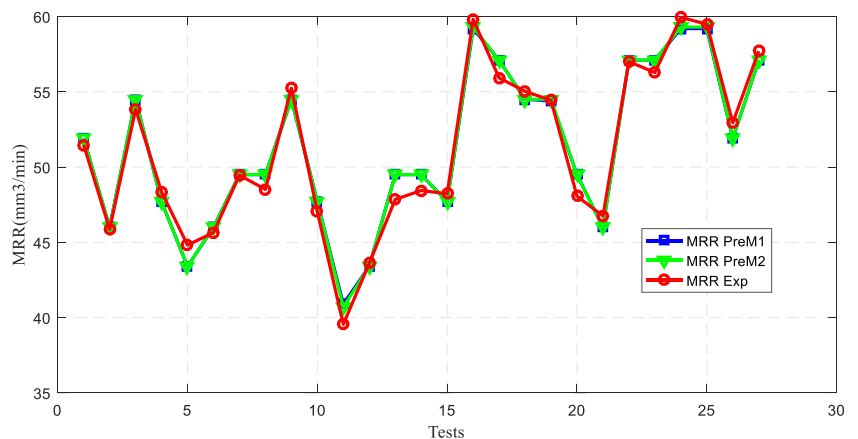
Fig. 28 Comparison of predicted and experimental material removal rate (MRR)
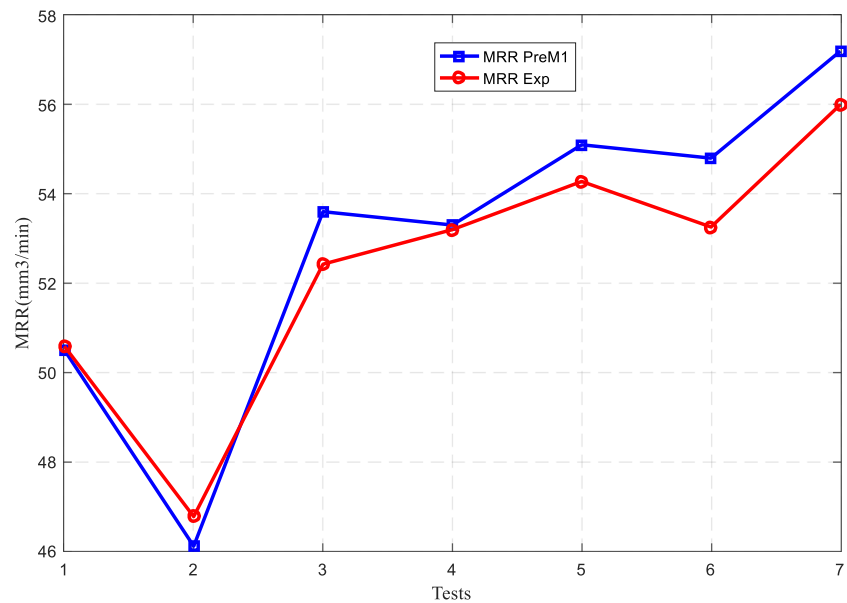
The influence of pulse on time on the MRR is shown in Fig. 41a and b.

Figure 41 b shows that increasing pulse on time results in a significant increase in MRR. This figure also shows the largest increase in the MRR produced in the low current region. A high pulse on time transfers more discharge energy to the workpiece and therefore increases the removal rate of the material.

Figure 41c shows that the MRR turns out to be maximized in the region with a short pulse on time and maximum voltage values. Although the quantity of molten material will be small, but when the voltage is increased, the intensity of the electric field in the volume between the electrodes is greater than the resistance of the liquid dielectric (at least in certain places), which allows current to flow between the two electrodes. As a result, rapid tearing of the material is produced. This may be

due to an increase in the density of surface crack caused by the localized effect of limited heat dissipation. The most influential factor among the three machining parameters on the material removal rate is pulse on time with a maximum contribution of 28.37%

5.2 Tool wear rate

Figure 42 shows a graphical representation of the fuzzy tool wear rate (TWR) as a function of the three machining parameters.

Figure 42a shows a decrease in EWR with the increase in voltage. This returns according to P. Ong et al. [9] to the decrease of current participating in the removal of material. The decrease of current is caused by the formation of a viscous

Fig. 29 Variation of the experimental and predicted tool wear rate (TWR) as a function of the number of tests
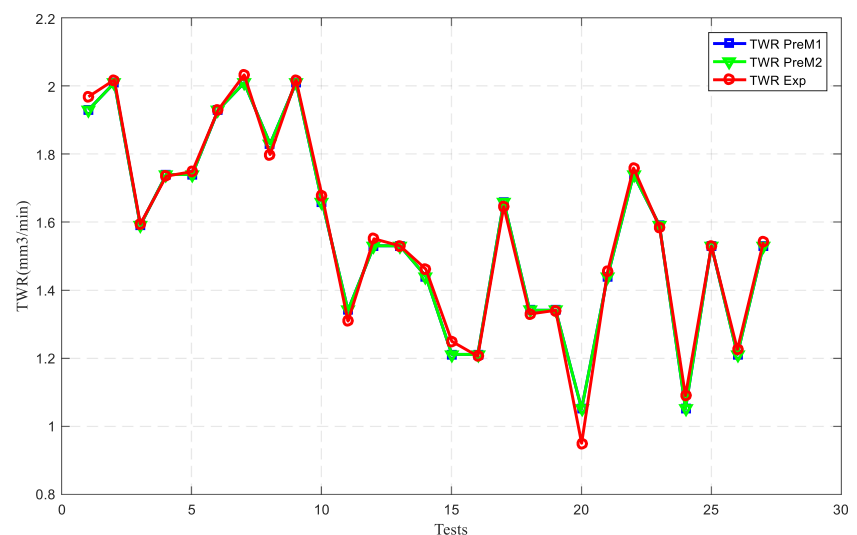
Fig. 30 Comparison of predicted and experimental tool wear rate (TWR)
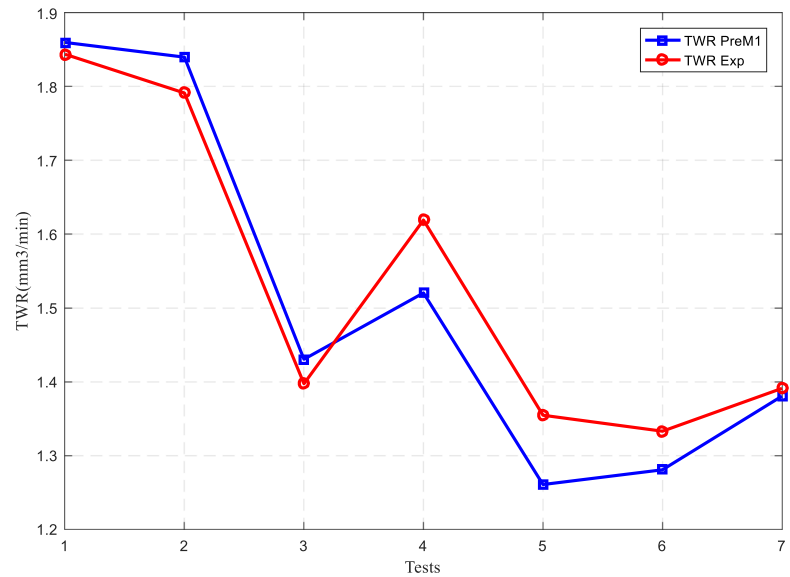
layer slowing the exchange of species in the environment of the electrode.

Figure 42b and c show that an increase in Pulse on time leads to a reduction in EWR. According to Y.C. Lin et al., [27] this is due to the deposition of the cracked pyrolytic carbon from the dielectric on the electrode, which leads to the formation of a protective layer. On the other hand, an increase in EWR is observed at currents greater than 14 A (Fig. 42b) and at small voltage values (Fig. 42c). This is due to the fact that the conductivity of the electrode is much higher than the conductivity of the room, and therefore, the heat given off by the electrode is faster which is indicated in the work of C.P. Mohanty [28].

The most influential factor among the three machining parameters on the tool wear rate (TWR) is the voltage with a maximum contribution of 39.80%.

5.3 Wear rate

Figure 43a, b, and c show the variation of WR. And as WR represents the ratio between the tool removal rate and the material removal rate, then its variation is explained by the same reasons for variation of MRR and TWR.

The most influential factor among the three machining parameters on the wear rate (EWR) is the voltage with a maximum contribution of 52.62%.

Fig. 31 Variation of the experimental and predicted wear rate (WR) as a function of the number of tests
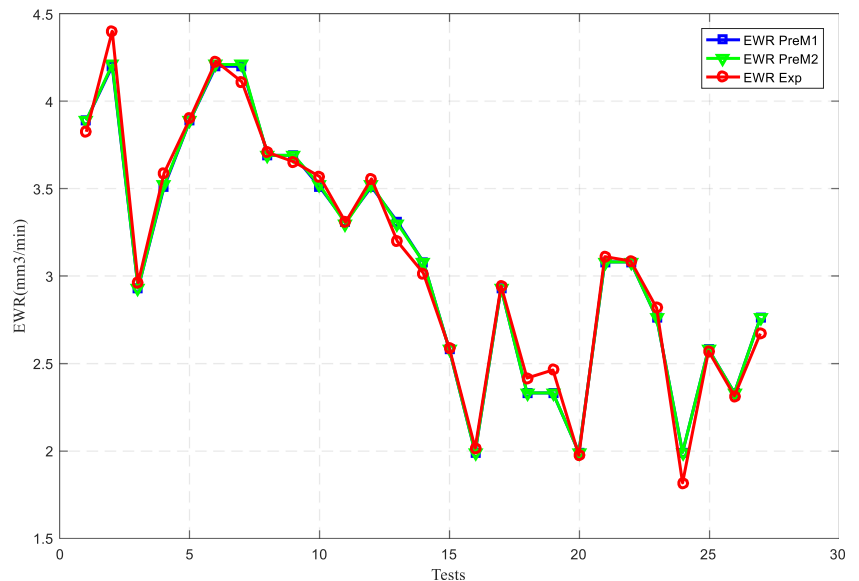
Fig. 32 Comparison of predicted and experimental wear rate (WR)
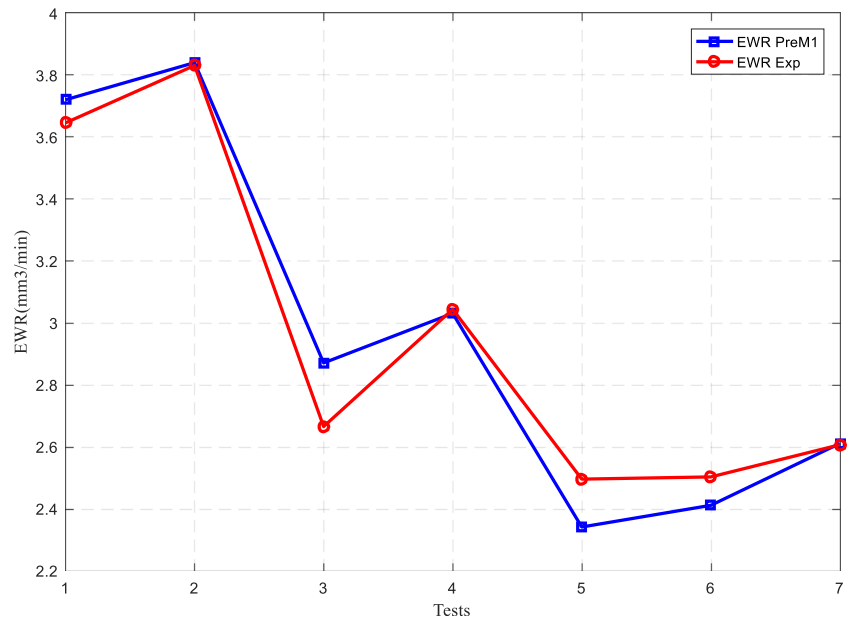
5.4 Surface roughness

Figure 44 graphically shows the effect of current (I), voltage (V), and pulse on time (Ton) on the surface roughness.

As seen in Fig. 44a, the surface plot consists of two regions: a high slope region and a low slope region. In the region with a low slope, the roughness of the surface gradually increases with the voltage. Also, in this region, the roughness increases with the increase of the current.

In the second region V > 160 V and I < 14 A, the roughness increases rapidly when the voltage increases due to surface damage, which is attributed to the formation of cracks. The increase of the current in this voltage range causes greater melting of the material which leads to a reduction in crack formation. Slowing the formation of cracks reduces the size and depth of craters generated due to the high thermal decomposition point of the part material; therefore, the roughness decreases.

Figure 44b clearly shows that the roughness of the surface is controlled by the current and pulse on time which is explained by the quantity of energy applied during the duration of the pulse. With a longer pulse on time and a high current, more material of the part will be melted. Increased discharge current causes impulsive

Fig. 33 Variation of the experimental and predicted surface roughness (Ra) as a function of the number of tests
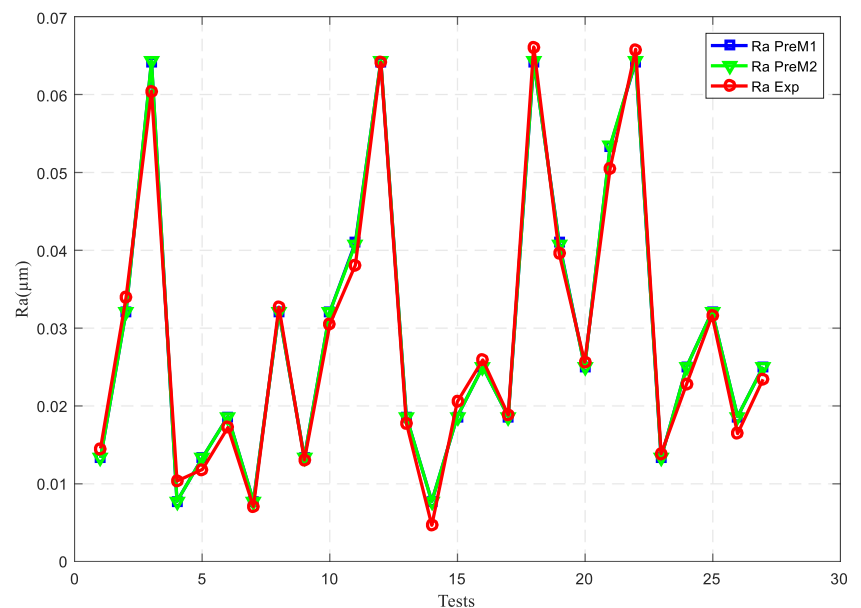
Fig. 34 Comparison of predicted and experimental surface roughness (Ra)
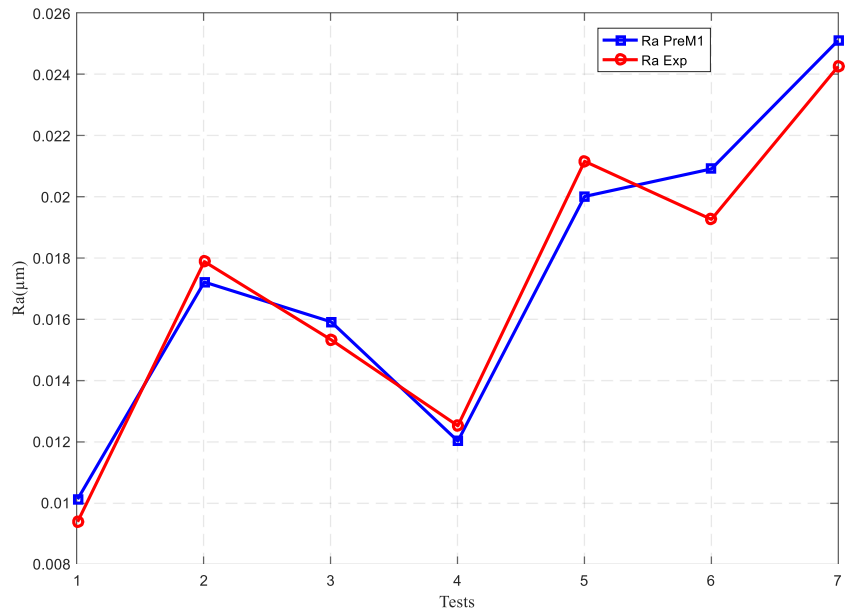
force acting on the workpiece. This improves the formation of a wider and deeper crater which will increase the surface roughness. On the other hand and despite the discharge time is important but the application of a low current caused less spark energy released. This led to the formation of tiny-sized craters on the machined surface and therefore caused a good surface finish this has been reported in the work of Rahul et al. [4].

Figure 44c shows that a combination of the low values of pulse on time and the average values of the voltage leads to maximum values of surface roughness.

The most influential factor among the three machining parameters on the surface roughness (Ra) is pulse on time with a maximum contribution of 81.24%.

5.5 Radial overcut

Figure 45 shows the evolution of radial overcut as a function of current, Volatge and Pulse on time.

Generally, we see that the value of radial overcut increases with Pulse on time.

Fig. 35 Variation of the experimental and predicted radial overcut (ROC) as a function of the number of tests
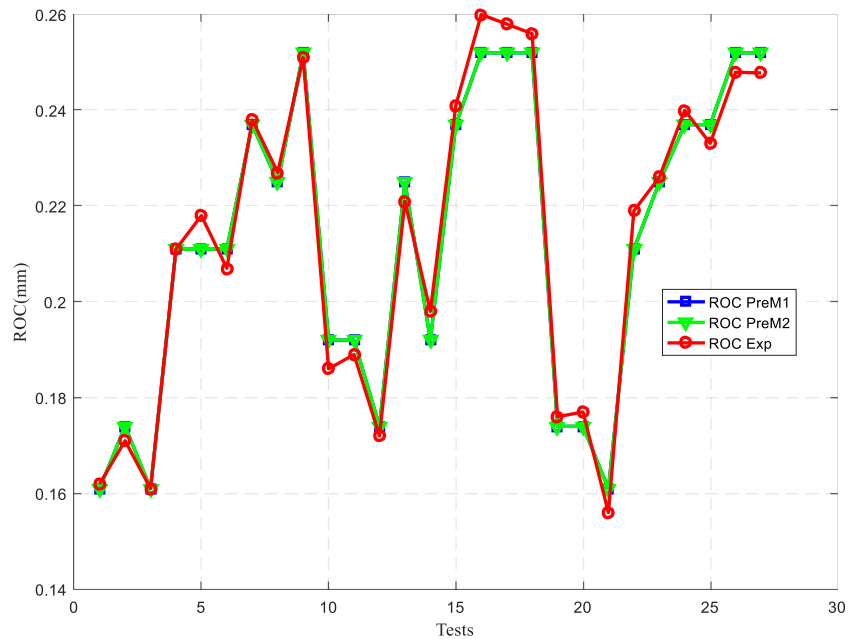
Fig. 36 Comparison of predicted and experimental radial overcut (ROC)
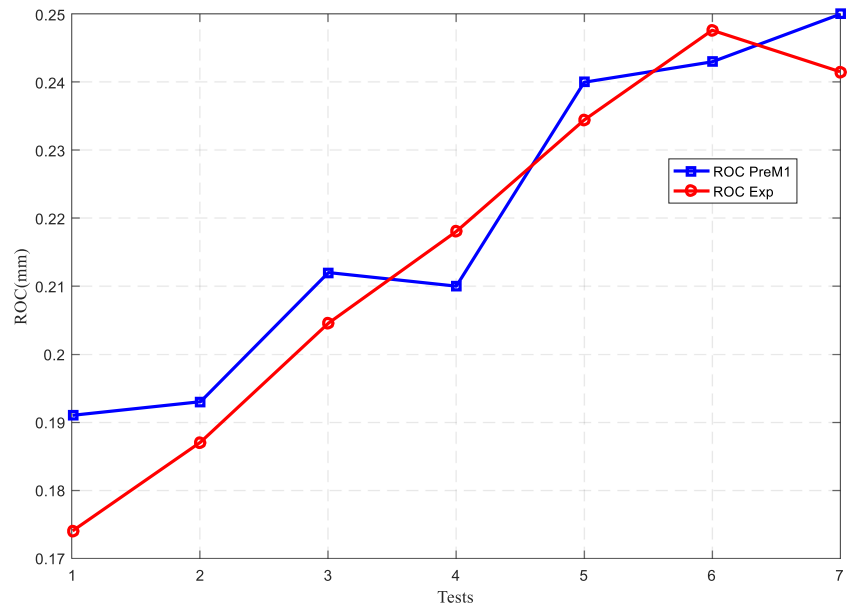
Figure 45a shows that radial overcut decreases with increasing current and voltage to a value of 14 A for current and a value of 160 V for voltage. Beyond these values, there is a slight increase in radial overcut.

Figure 45b shows that radial overcut increases with increasing pulse on time regardless of the current value; this increase according to Dhar et al. [29] is due to the prolonged presence of sparks thus producing an increase in energy per spark.

A combination of the maximum values of voltage and pulse on time leads to maximum values of radial overcut as shown in Fig. 45c.

The most influential factor among the three machining parameters on the radial overcut (ROC) is pulse on time with a maximum contribution of 36.11%.

5.6 Circularity

Figure 46 shows the evolution of circularity as a function of current, voltage, and pulse on time.

In general, as shown in Fig. 46a and b, the precise tolerance of circularity is obtained for mean values of three variables (I = 14 A, V = 160 V, and Ion = 200 μs).

Fig. 37 Variation of the experimental and predicted circularity (CIR) as a function of the number of tests
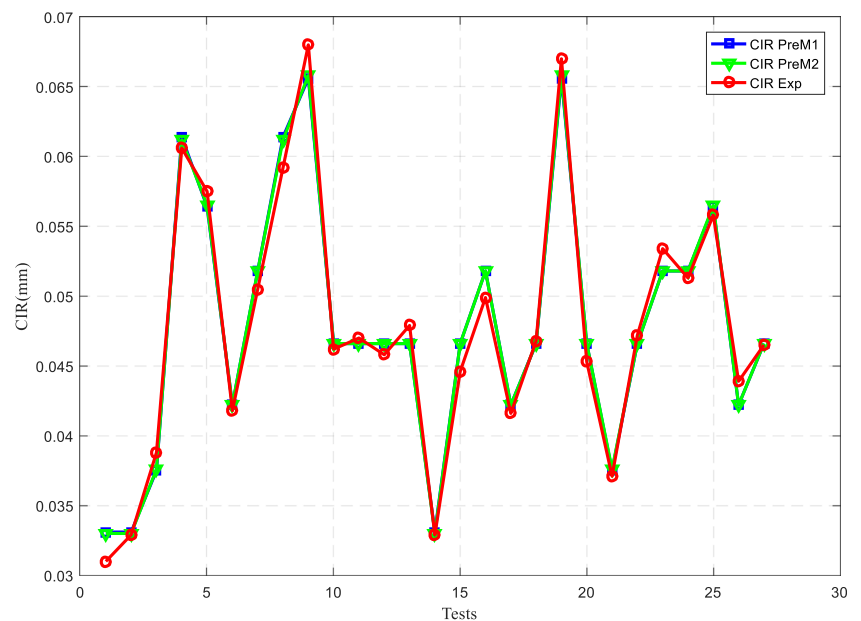
**Fig. 38** Comparison of predicted and experimental circularity (CIR)
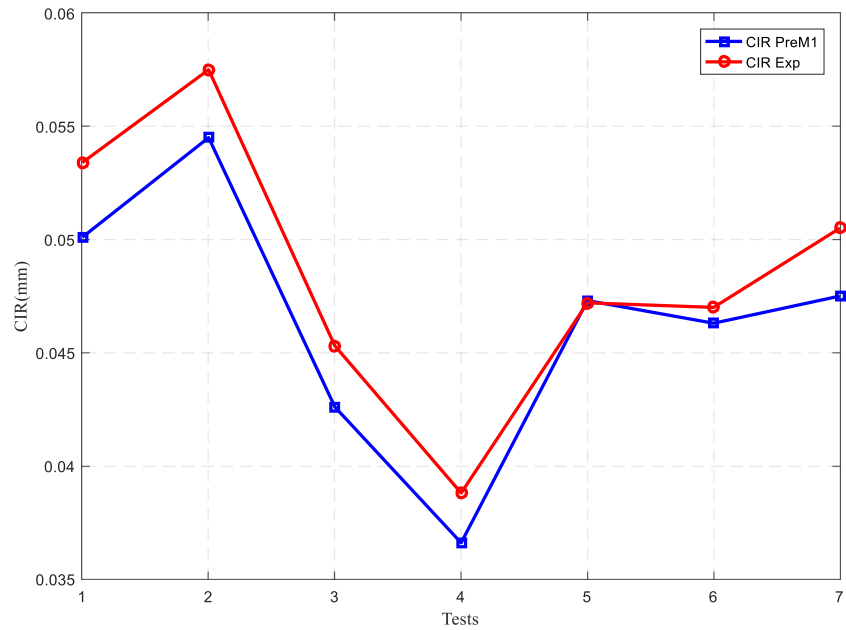
As shown in Fig. 46c, the combination of maximum pulse on time values and minimum voltage values leads to an increase in the tolerance of circularity.

The most influential factor among the three machining parameters on circularity (CIR) is the voltage with a maximum contribution of 49.54%.

5.7 Cylindricity

Figure 47 shows the evolution of cylindricity as a function of current, voltage, and pulse on time.

The combination of the minimum values of voltage and pulse on time with maximum values of the current leads to a minimum cylindricity as illustrated in Figs. 47a, b. The increase in pulse on time and voltage leads to a rapid increase in cylindricity up to a voltage of 160 Volts. Above this value, the cylindricity stabilizes (Fig. 47c).

An increase in the pulse duration results in deterioration of the lateral side of the hole due to the recoat layer formed on the lateral face of the hole, for which the surface quality deteriorates, and consequently the increase in cylindricity. This is due, according to Ay

Fig. 39 Variation of the experimental and predicted cylindricity (CYL) as a function of the number of tests
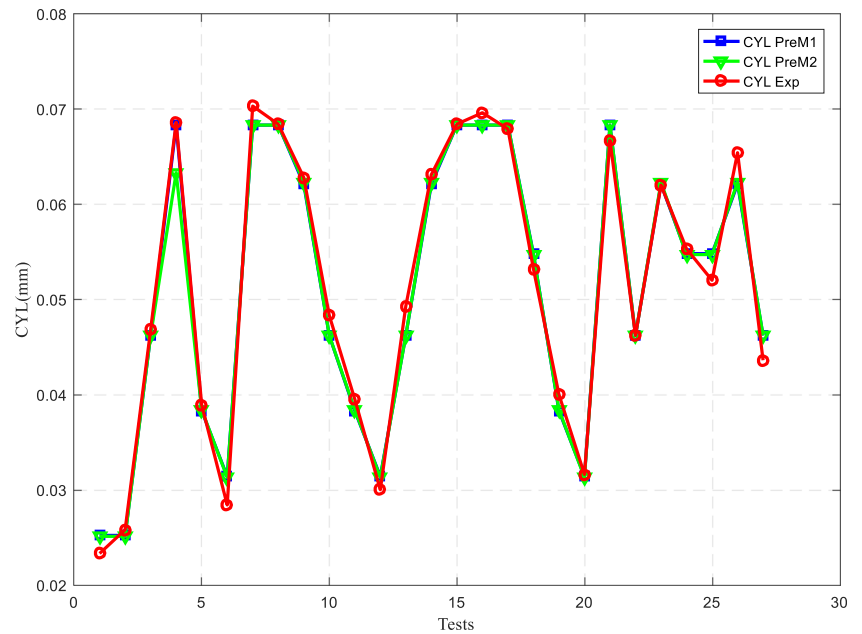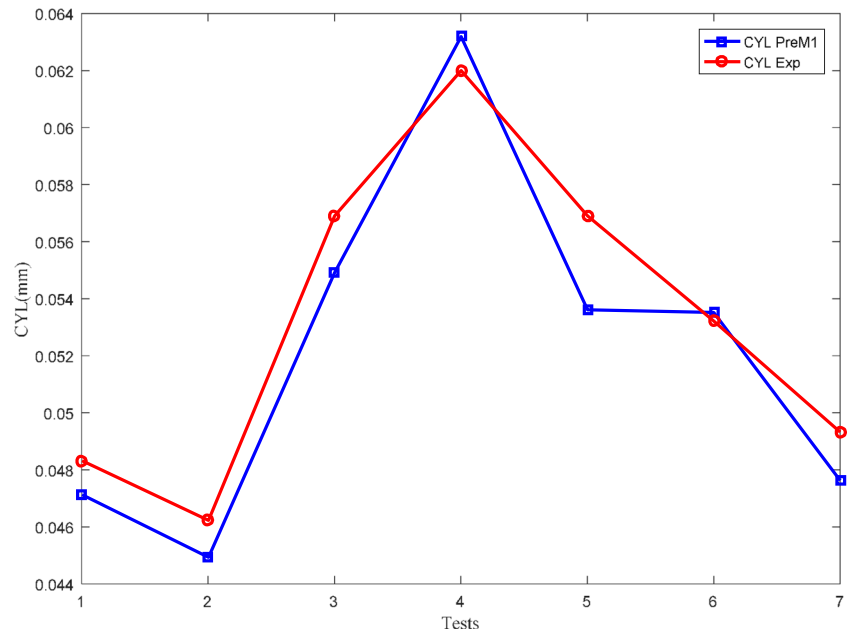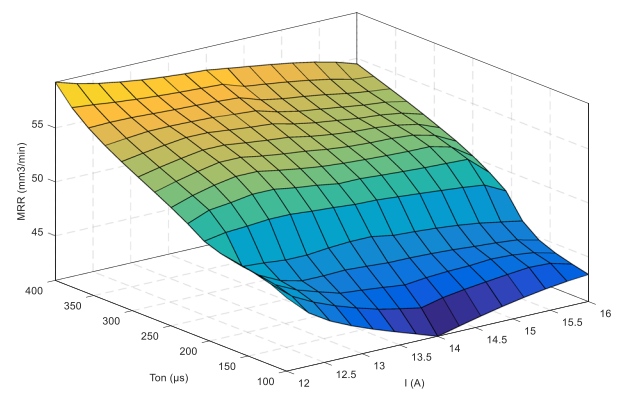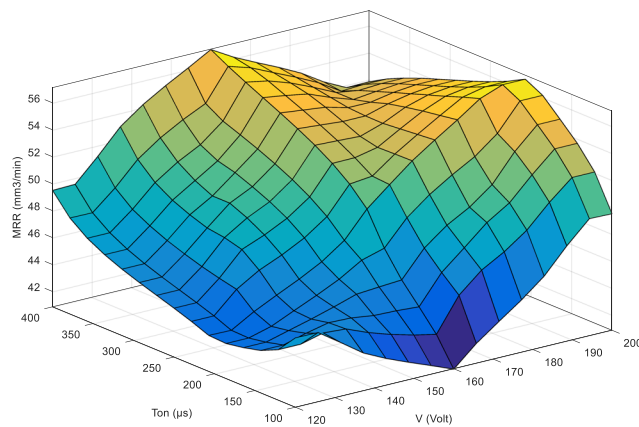
Fig. 40 Comparison of predicted and experimental cylindricity (CYL)
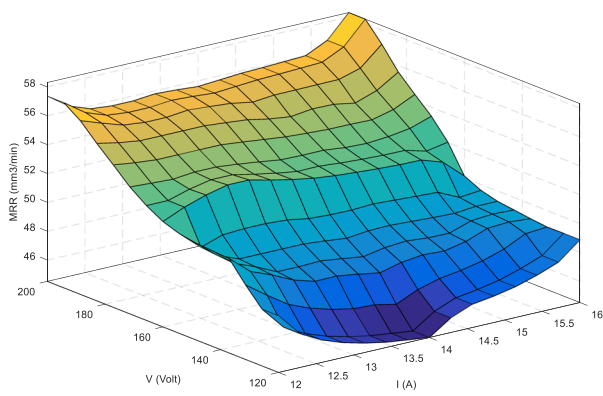
(a)

(b)

(c)

Fig. 41 Variation of the material removal rate predicted by fuzzy logic according to the machining parameters
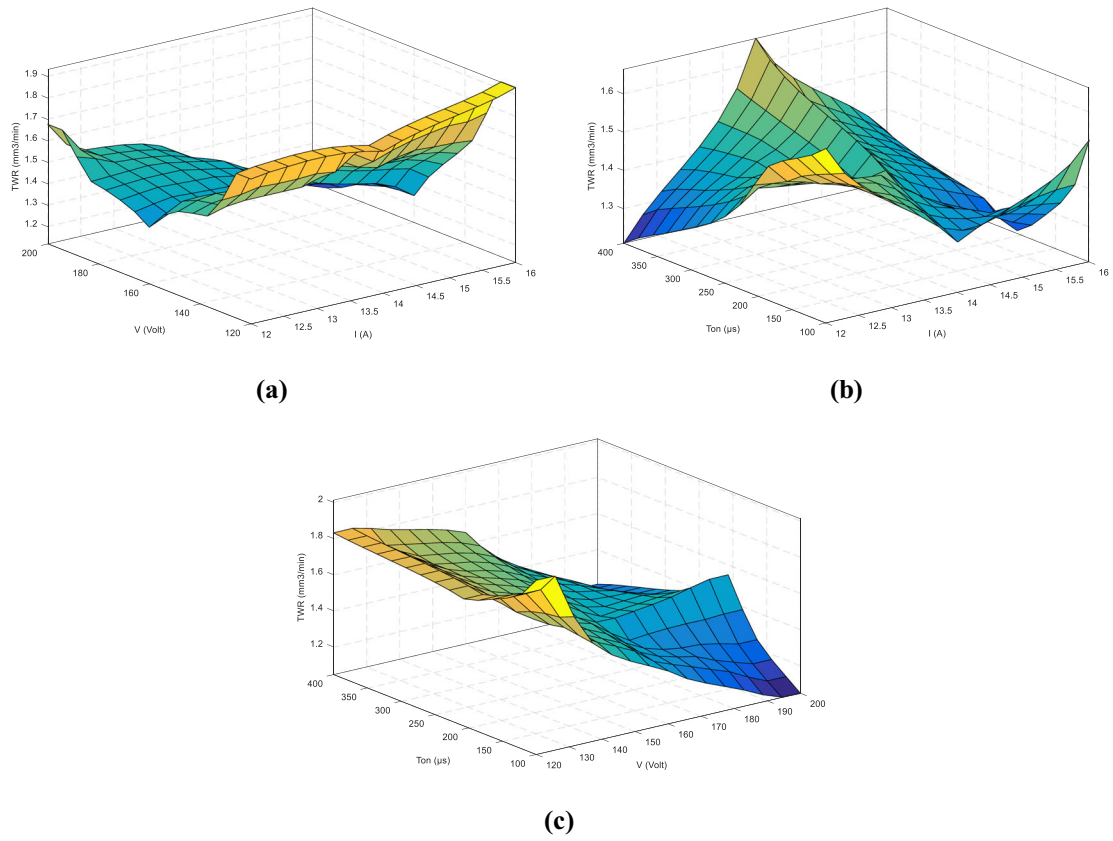
(a)

(b)

(c)

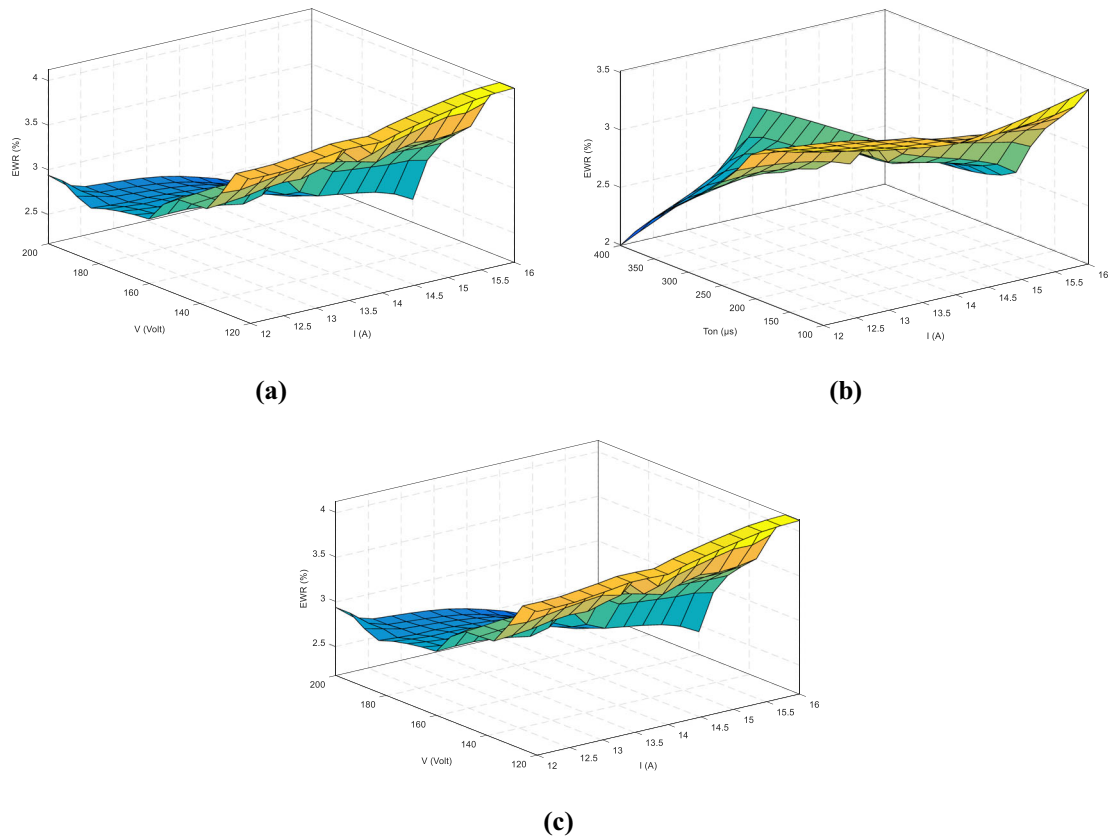Fig. 42 Variation of the tool wear rate predicted by fuzzy logic according to the machining parameters

(a)

(b)

(c)

Fig. 43 Variation of the wear rate predicted by fuzzy logic according to the machining parameters
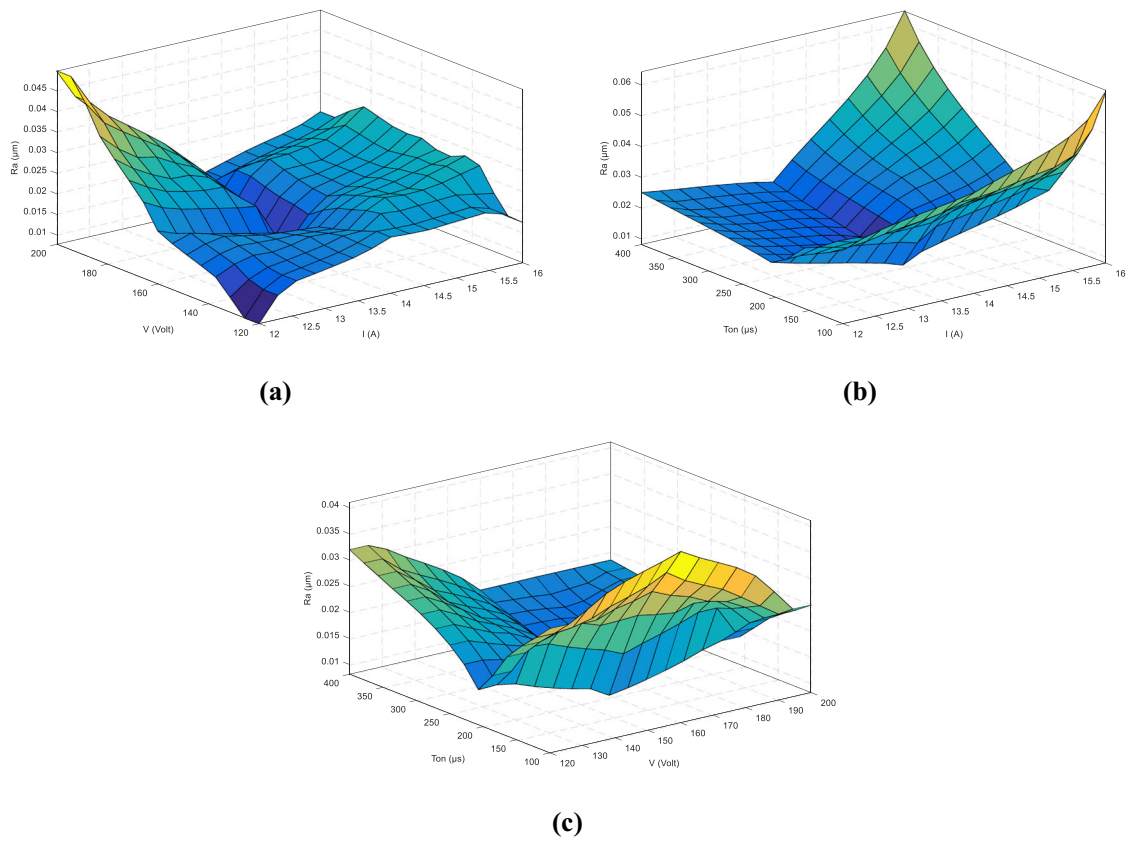
Fig. 44 Variation of the surface roughness predicted by fuzzy logic according to the machining parameters
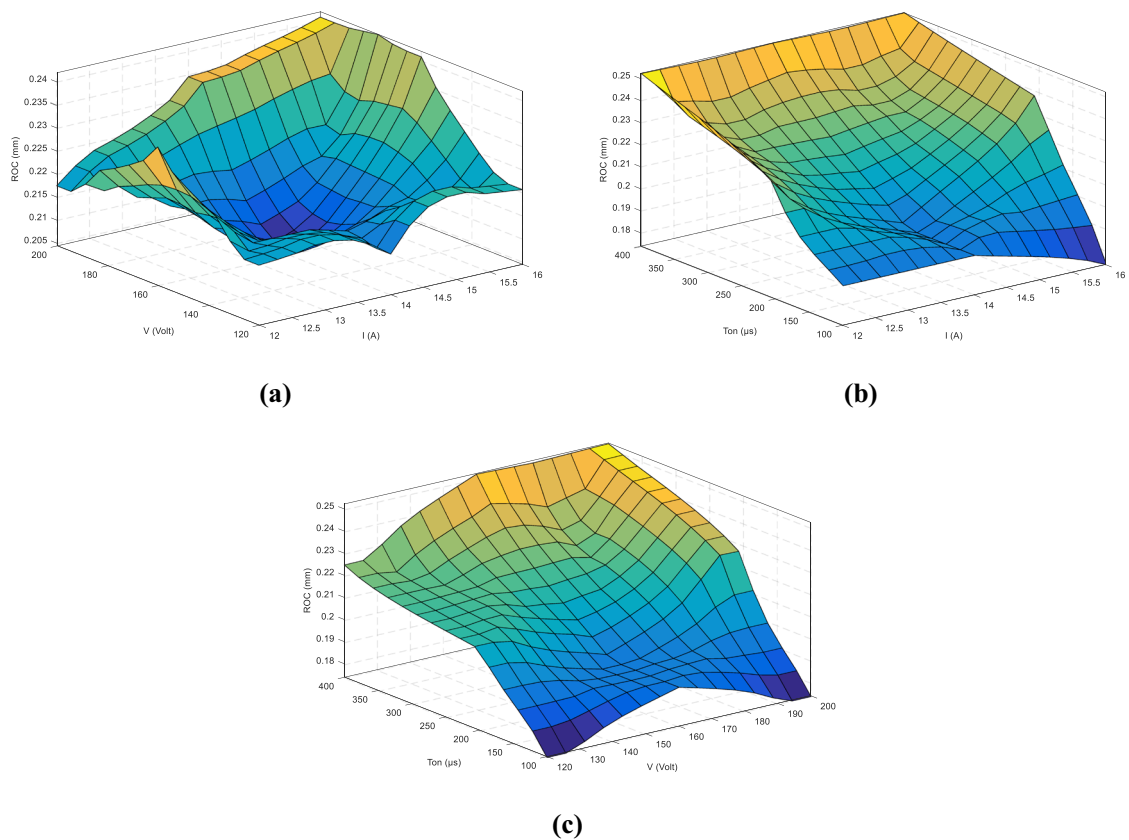

Fig. 45 Variation of the radial overcut predicted by fuzzy logic according to the machining parameters
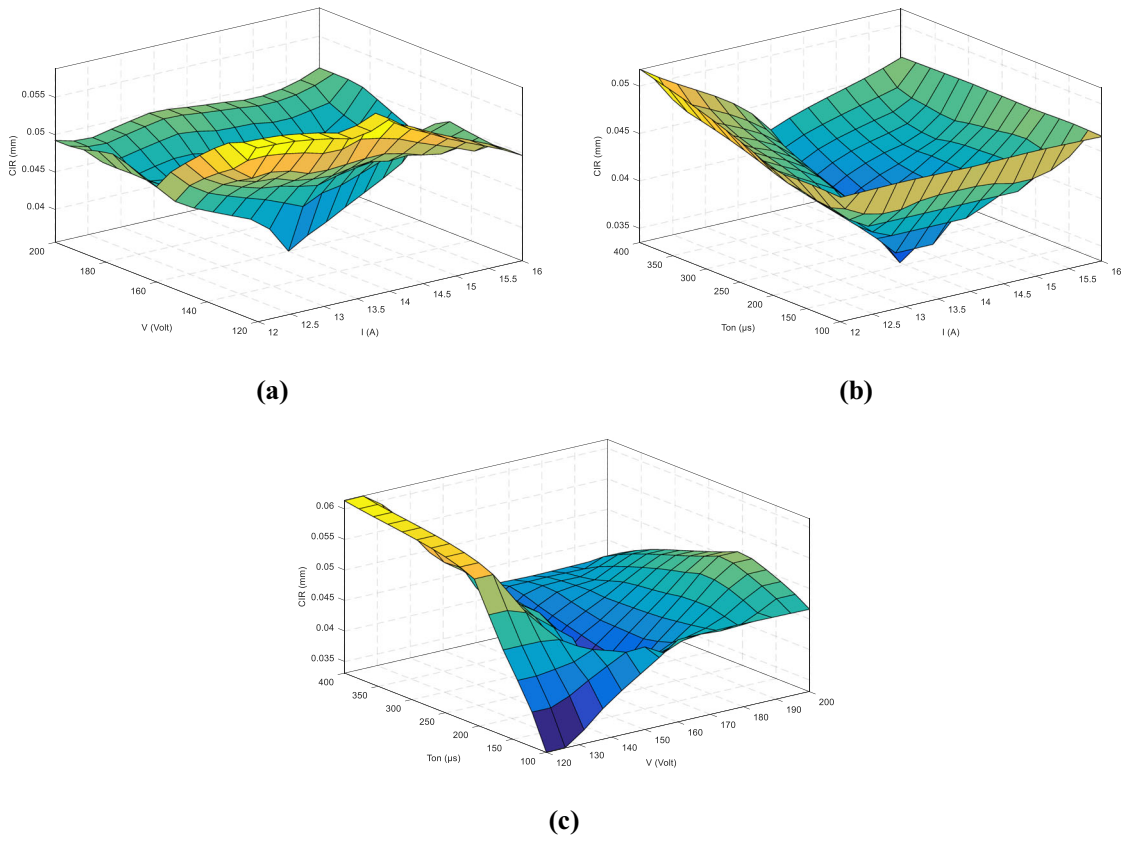
(a)

(b)

(c)

Fig. 46 Variation of the circularity predicted by fuzzy logic according to the machining parameters
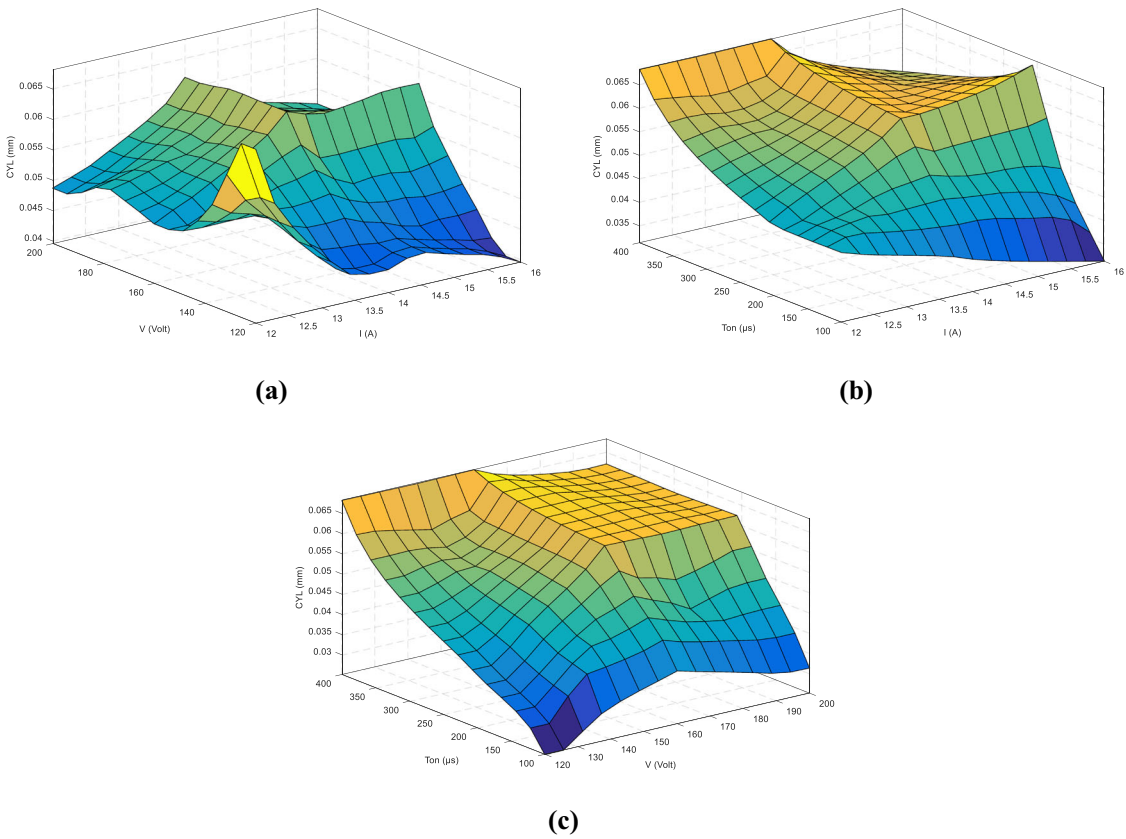

(a)

(b)

(c)

Fig. 47 Variation of the cylindricity predicted by fuzzy logic according to the machining parameters

et al. [18], to the higher discharge energy causing violent sparks and a resulting deeper erosion crater on the surface.

The most influential factor among the three machining parameters on the cylindricity (CYL) is pulse on time with a maximum contribution of 63.10%.

6 Conclusions

In the present work, an experimental study of the electrical discharge machining process (EDM) is carried out on AISI 1095 treated steel parts. The factors considered in this study are current (I), voltage (V), and pulse on time (Ton). Several conclusions are summarized as follows:

The experimental approach used in this work to measure the performance of electrical discharge machining (EDM) and the associated geometric errors can be used in a practical way. It is useful to be an economical way to follow the machining performance evolution of AISI 1095 treated steel with EDM.

The experimental approach for measuring the electrical discharge machining performance and the associated geometric errors is easy to implement and use. The response of the measurement system to the nature of the machining operation is adequate and the results show that the machining performance has been measured satisfactorily whatever the machining conditions used.

The membership functions and the fuzzy rules developed were based on experimental measurements of the machining electrical discharge performance and associated geometric errors.

The effects of the machining parameters, on the electrical discharge machining performance and the associated geometric errors, have been studied and it has been found that certain cutting parameters have a greater effect than others such as follows:

– The most influential factor among the three machining parameters on the material removal rate is pulse on time with a maximum contribution of 28.37%.
– The most influential factor among the three machining parameters on the tool wear rate (TWR) is the voltage with a maximum contribution of 39.80%.
– The most influential factor among the three machining parameters on the wear rate (WR) is the voltage with a maximum contribution of 52.62%.
– The most influential factor among the three machining parameters on the surface roughness (Ra) is pulse on time with a maximum contribution of 81.24%.
– The most influential factor among the three machining parameters on the radial overcut (ROC) is pulse on time with a maximum contribution of 36.11%.

– The most influential factor among the three machining parameters on circularity (CIR) is the voltage with a maximum contribution of 49.54%.
– The most influential factor among the three machining parameters on the cylindricity (CYL) is pulse on time with a maximum contribution of 63.10%.

The suitability of the fuzzy model has been checked and found adequate with a level of precision of 98.489% for material removal rate (MRR), 96.614% for tool wear rate (TWR), 97.076% for wear rate (WR), 94.715% for surface roughness (Ra), 95.996% for radial overcut (ROC), 95.619% for circularity (CIR), and 97.063% for cylindricity (CYL) which demonstrates that the model can be used to predict the electrical discharge machining performance of AISI 1095 treated steel.

The comparison and validation of the fuzzy results with the results of the experimental tests confirmed the high accuracy of the model. The fuzzy modeling technique could be an economical and effective method for predicting other electrical discharge machining (EDM) performance.

The strategy based on operator qualification to select the machining parameters for machining AISI 1095 treated steel can be described by fuzzy set theory.

References

1. Dhanabalan S, Sivakumar K, Narayanan CS (2015) Experimental investigation on electrical discharge machining of titanium alloy using copper, brass and aluminum electrodes. J Eng Sci Technol 10(1):72–80
2. Torres A, Puertas I, Luis CJ (2016) EDM machinability and surface roughness analysis of INCONEL 600 using graphite electrodes. Int J Adv Manuf Technol 84(9–12):2671–2688. https://doi.org/10.1007/s00170-015-7880-x
3. Fazlollahtabar H, Gholizadeh H (2020) Fuzzy possibility regression integrated with fuzzy adaptive neural network for predicting and optimizing electrical discharge machining parameters. Comput Ind Eng 140:106225. https://doi.org/10.1016/j.cie.2019.106225
4. Rahul DS, Biswal BB, Mahapatra SS (2019) Machinability analysis of Inconel 601, 625, 718 and 825 during electro-discharge machining: on evaluation of optimal parameters setting. Measurement. 137:382–400. https://doi.org/10.1016/j.measurement.2019.01.065
5. Hanif M, Ahmad W, Hussain S, Jahanzaib M, Shah AH (2019) Investigating the effects of electric discharge machining parameters on material removal rate and surface roughness on AISI D2 steel using RSM-GRA integrated approach. Int J Adv Manuf Technol 101:1255–1265. https://doi.org/10.1007/s00170-018-3019-1
6. Pradhan MK, Biswas CK (2010) Neuro-Fuzzy and neural network-based prediction of various responses in electrical discharge machining of AISI D2 steel. Int J Adv Manuf Technol 50(5):591–610. https://doi.org/10.1007/s00170-010-2531-8
7. Khan AA (2008) Electrode wear and material removal rate during EDM of aluminum and mild steel using copper and brass

electrodes. Int J Adv Manuf Technol 39:482–487. https://doi.org/10.1007/s00170-007-1241-3

8. Shen Y, Liu Y, Dong H, Zhang K, Lv L, Zhang X, Zheng C, Ji R (2017) Parameters optimization for sustainable machining of Ti–6Al–4V using a novel high-speed dry electrical discharge milling. Int J Adv Manuf Technol 90(9):2733–2740. https://doi.org/10.1007/s00170-016-9600-6

9. Ong P, Chong CH, Bin Rahim MZ, Lee WK, Sia CK, Bin Ahmad MAH (2020) Intelligent approach for process modelling and optimization on electrical discharge machining of polycrystalline diamond. J Intell Manuf 31:227–247. https://doi.org/10.1007/s10845-018-1443-6

10. Newton TR, Melkote SN, Watkins TR, Trejo RM, Reister L (2009) Investigation of the effect of process parameters on the formation and characteristics of recast layer in wire-EDM of Inconel 718. Mater Sci Eng A 513-514:208–215. https://doi.org/10.1016/j.msea.2009.01.061

11. Rajesha S, Sharma A, Kumar P (2010) Some aspects of surface integrity study of electro discharge machined Inconel 718. In: Hinduja S, Li L (eds) Proceedings of the 36th international MATADOR conference. Springer, London. https://doi.org/10.1007/978-1-84996-432-6_98

12. Zhang JH, Lee TC, Lau WS (1997) Study on the electro-discharge machining of a hot pressed aluminum oxide based ceramic. J Mater Process Technol 63(1–3):908–912. https://doi.org/10.1016/S0924-0136(96)00012-X

13. Kiyak M, Çakır O (2007) Examination of machining parameters on surface roughness in EDM of tool steel. J Mater Process Technol 191(1–3):141–144. https://doi.org/10.1016/j.jmatprotec.2007.03.008

14. Lee HT, Hsu FC, Tai TY (2004) Study of surface integrity using the small area EDM process with a copper–tungsten electrode. Mater Sci Eng A 364(1–2):346–356. https://doi.org/10.1016/j.msea.2003.08.046

15. Rebelo JC, Dias AM, Mesquita R, Vassalo P, Santos M (2000) An experimental study on electro-discharge machining and polishing of high strength copper–beryllium alloys. J Mater Process Technol 103(3):389–397. https://doi.org/10.1016/S0924-0136(99)00492-6

16. Raj S, Kumar K (2015) Optimization and prediction of material removing rate in die sinking electro discharge machining of EN45 steel tool. Mater Today 2(4–5):2346–2352. https://doi.org/10.1016/j.matpr.2015.07.296

17. Vikas RAK, Kumar K (2014) Effect and optimization of various machine process parameters on the surface roughness in EDM for an EN41 material using Grey-Taguchi. Procedia Mater Sci 6:383–390. https://doi.org/10.1016/j.mspro.2014.07.049

18. Ay M, Caydas U, Hascalik A (2013) Optimization of micro-EDM drilling of Inconel 718 superalloy. Int J Adv Manuf Technol 66:1015–1023. https://doi.org/10.1007/s00170-012-4385-8

19. Singh S (2012) Optimization of machining characteristics in electric discharge machining of 6061Al/Al2O3p/20P composites by grey relational analysis. Int J Adv Manuf Technol 63:1191–1202. https://doi.org/10.1007/s00170-012-4148-6

20. Chen YF, Lin YJ, Lin YC, Chen SL, Hsu LR (2010) Optimization of electrodischarge machining parameters on ZrO2 ceramic using the Taguchi method. Proc Instit Mech Eng B J Eng Manuf 224(2):195–205. https://doi.org/10.1243/09544054JEM1437

21. Chiang KT (2008) Modeling and analysis of the effects of machining parameters on the performance characteristics in the EDM process of Al2O3 + TiC mixed ceramic. Int J Adv Manuf Technol 37:523–533. https://doi.org/10.1007/s00170-007-1002-3

22. Tzeng YF (2008) Development of a flexible high-speed EDM technology with geometrical transform optimization. J Mater Process Technol 203:355–364. https://doi.org/10.1016/j.jmatprotec.2007.10.034

23. Keskin Y, Halkaci HS, Kizil M (2006) An experimental study for determination of the effects of machining parameters on surface roughness in electrical discharge machining (EDM). Int J Adv Manuf Technol 28:1118–1121. https://doi.org/10.1007/s00170-004-2478-8

24. Grigor'ev SN, Kuzin VV, Fedorov SY, Szalay T, Farkas B (2015) Technological aspects of the electrical-discharge machining of small-diameter holes in a high-density ceramic. Part 2. Refract Ind Ceram 55:469–472. https://doi.org/10.1007/s11148-015-9746-z

25. Muthukumar V, Rajesh N, Venkatasamy R, Sureshbabu A, Senthilkumar N (2014) Mathematical modeling for radial overcut on electrical discharge machining of Incoloy 800 by response surface methodology. Procedia Mater Sci 6:1674–1682. https://doi.org/10.1016/j.mspro.2014.07.153

26. Klocke F, Schwade M, Klink A, Veselovac D (2013) Analysis of material removal rate and electrode wear in sinking EDM roughing strategies using different graphite grades. Procedia CIRP 6:163–167. https://doi.org/10.1016/j.procir.2013.03.079

27. Lin YC, Lee HS (2008) Machining characteristics of magnetic force-assisted EDM. Int J Mach Tools Manuf 48(11):1179–1186. https://doi.org/10.1016/j.ijmachtools.2008.04.004

28. Mohanty CP, Mahapatra SS, Singh MR (2017) An intelligent approach to optimize the EDM process parameters using utility concept and QPSO algorithm. Eng Sci Technol Int J 20(2):552–562. https://doi.org/10.1016/j.jestch.2016.07.003

29. Dhar S, Purohit R, Saini N, Akhil S, Kumar GH (2007) Mathematical modeling of electric discharge machining of cast Al–4Cu–6Si alloy–10wt.% SiCP composites. J Mater Process Technol 194(1–3):24–29. https://doi.org/10.1016/j.jmatprotec.2007.03.121